Journal of Computational Physics 555 (2026) 114786

Contents lists available at ScienceDirect

Journal of Computational Physics

journal homepage: www.elsevier.com/locate/jcp

On a class of higher-order length preserving and energy decreasing IMEX schemes for the Landau-Lifshitz equation ⋆

Xiaoli Li [a], Jie Shen [b,*], Nan Zheng [c]

[a] School of Mathematics, Shandong University, 250100, Jinan Shandong, P.R. China
[b] Corresponding Author. School of Mathematical Science, Eastern Institute of Technology, Ningbo, China
[c] Department of Applied Mathematics, The Hong Kong Polytechnic University, Hung Hom, Kowloon, Hong Kong

ARTICLE INFO

2000 MSC:
35Q56
65M12
65M15

Keywords:
Landau-Lifshitz equation
Length preserving
Higher-order
Stability
Error estimates
Time discretization

ABSTRACT

We construct new higher-order implicit-explicit (IMEX) and semi-implicit schemes using the generalized scalar auxiliary variable (GSAV) approach for the Landau-Lifshitz equation. These schemes are linear, length preserving, and require solving either: (a) decoupled elliptic equations with constant coefficients, when the nonlinear term is treated fully explicitly, or (b) a coupled elliptic system with variable coefficients, when the nonlinear term is treated semi-implicitly. We show that numerical solutions of these schemes are uniformly bounded without any restriction on the time step size, and establish rigorous error estimates in $l^\infty(0,T;H^1(\Omega))\bigcap l^2(0,T;H^2(\Omega))$ of orders 1 to 5 in a unified framework. Ample numerical examples, including some challenging benchmark problems, are presented to validate the accuracy and robustness of the proposed schemes.

1. Introduction

Magnetization dynamics in a ferromagnetic material occupying a region Ω is governed by the Landau-Lifshitz equation [1–4]:

$$\frac{\partial \mathbf{m}}{\partial t} = -\beta \mathbf{m}\times\Delta\mathbf{m} - \gamma\mathbf{m}\times(\mathbf{m}\times\Delta\mathbf{m}), \quad \text{in } \Omega\times J, \tag{1.1}$$

with

$$\mathbf{m}(\mathbf{x},0)=\mathbf{m}_0(\mathbf{x}),\ \text{with } |\mathbf{m}_0(\mathbf{x})|=1,\ \text{in } \Omega, \tag{1.2}$$

subject to either homogeneous Neumann or periodic boundary conditions. In the above, $\mathbf{m}=(m_1,m_2,m_3)^t$ describes the magnetization in continuum ferromagnets, Ω is an open bounded domain in $\mathbb{R}^d$ with $d\in\{1,2,3\}$, J denotes $(0,T]$ for some $T>0$, $\gamma>0$ is the Gilbert damping parameter and β is an exchange parameter. When $\beta\neq 0$, it is often referred to as the Landau-Lifshitz-Gilbert equation. The solution of (1.1) preserves pointwisely its magnitude, i.e.,

$$\frac{\mathrm{d}}{\mathrm{d}t}|\mathbf{m}(\mathbf{x},t)|^2=0, \tag{1.3}$$

⋆ This work is supported by the National Natural Science Foundation of China grants 12271302, 12371409, W2431008 and 12131014 and Shandong Provincial Natural Science Foundation for Outstanding Youth Scholar (Grant No. ZR2024JQ030), and the Hong Kong Polytechnic University Postdoctoral Research Fund 1-W22P.

* Corresponding author.
E-mail addresses: xiaolimath@sdu.edu.cn (X. Li), jshen@eitech.edu.cn (J. Shen), znan2017@163.com (N. Zheng).

https://doi.org/10.1016/j.jcp.2026.114786
Received 13 June 2025; Received in revised form 10 December 2025; Accepted 16 February 2026
Available online 18 February 2026
0021-9991/

which, together with (1.2), implies that $|\mathbf{m}(\mathbf{x},t)| = 1,\ \forall(\mathbf{x},\ t)$. It also satisfies the following energy dissipation law:

$$\frac{\mathrm{d}E}{\mathrm{d}t} = -\gamma\|\mathbf{m}\times\Delta\mathbf{m}\|^2, \quad \text{with } \ E = \frac{1}{2}\int_\Omega |\nabla\mathbf{m}|^2\ d\mathbf{x}. \tag{1.4}$$

The Landau-Lifshitz equation is a fundamental equation in physics, and its accurate and efficient numerical simulation plays an important role in understanding both the statics and dynamics in ferromagnetic materials [5–7], and has attracted much attention in the past decades, [8–13] and the references therein.

Since $|\mathbf{m}(\mathbf{x},t)| = 1$ holds under the initial condition $|\mathbf{m}_0(\mathbf{x})| = 1$, it is important to construct numerical schemes to satisfy these point-wise constraints at the discrete level. There are essentially three different strategies to deal with this constraint. (i) Penalty method [14,15]: introducing a suitable penalty term in the original equation to relax the point-wise constraint. This approach has been widely used in the numerical simulation for liquid crystal flows [16,17]. Main drawbacks of this approach are: it does not enforce the length constraint exactly, and it is challenging to numerically deal with the penalized formulation. (ii) Projection method [8,18]: projecting the intermediate magnetization $\tilde{\mathbf{m}}^{n+1}$ onto the unit sphere $\tilde{\mathbf{m}}^{n+1}/|\tilde{\mathbf{m}}^{n+1}|$ after solving the equation at every time level. This approach is very simple to implement, and has been frequently used [10,11,13,19,20]. However, it is difficult to enforce energy dissipation and to construct higher-order schemes especially combined with finite element method in space. (iii) Lagrange multiplier method: introducing a Lagrange multiplier to enforce the length constraint [7]. The simplest version of this approach is equivalent to a projection method, but their higher-order versions are different. This approach is easy to implement, and capable to enforce energy dissipation at the expense of solving one nonlinear algebraic equation. But its error analysis appears to be difficult.

Error analysis of numerical schemes for the Landau-Lifshitz equation (1.1) is difficult due to its highly nonlinear nature and the length constraint. E and Wang established a first-order error estimate for the projection scheme in [8]. On the other hand, Gui, Li and Wang [13] derived an optimal-order error estimate for a linearly implicit, lumped mass FEM on rectangular mesh under the condition $\Delta t \ge \kappa h^{r+1}$ for some $r > 1$, where κ is any positive constant. In addition, Cai et al. [21] established rigorous error estimates of the second-order and linear scheme for the Landau-Lifshitz equation with large damping parameters.

There are a number of equivalent formulations of the Landau-Lifshitz equation. An interesting formulation is

$$\alpha\partial_t\mathbf{m} + \mathbf{m}\times\partial_t\mathbf{m} = (I - \mathbf{m}\mathbf{m}^T)\Delta\mathbf{m}, \tag{1.5}$$

where α is a damping parameter which can be expressed in terms of $\beta,\ \gamma$. An advantage of this formulation is that its nonlinear term is easier to treat in error analysis, but on the other hand, it is more complicated to implement numerically. Akrivis et al. [12] constructed linearly implicit time discretizations up to order 5 combined with higher-order non-conforming finite elements in space, which satisfy a discrete energy dissipation law but do not ensure normalization of the magnetization. Alouges et al. [9,22,23] proposed the tangent plane schemes with first-order in time and provided a proof of convergence toward a weak solution. We refer to [9,12,22–24] and the references therein for more details on numerical approximations of (1.5).

The main purpose of this paper is to construct a new class of high-order IMEX schemes for the Landau-Lifshitz equation, with a generalized scalar auxiliary variable (GSAV) approach [25] to satisfy a (modified) energy dissipation law, and with a projection approach to preserve the pointwise length constraint, and to carry out a rigorous error analysis. Our main contributions are:

- The new schemes enjoy the following advantages: (i) they are purely linear, and at each time step only require solving (a) decoupled elliptic equations with constant coefficients when the nonlinear term is treated fully explicitly, or (b) a coupled elliptic system with variable coefficients when the nonlinear term is treated semi-implicitly; (ii) they preserve the pointwise length constraint; (iii) they satisfy a (modified) energy dissipation law, and their solutions are uniformly bounded.
- We carry out a rigorous error analysis for the semi-discretized schemes up to fifth-order in a unified framework and establish error estimates in $l^\infty(0,T;H^1(\Omega))\bigcap l^2(0,T;H^2(\Omega))$ for the magnetization field under a mild condition on the exchange parameter β if $\beta \neq 0$, and on $\Delta t \le (1+2^{q+1}C_0^q)^{-1}$, where C_0 is a positive constant and q is the order of numerical scheme (except that $q = 2$ for the first-order scheme).

To the best of the authors' knowledge, these are the first error estimates for higher-order numerical schemes which enforce normalization of the magnetization for the Landau-Lifshitz equation (1.1). Note that these estimates are established for the semi-discretized (in time) schemes, but it is expected that error estimates for consistent fully discretized schemes can be derived without severe time step constraints.

The paper is organized as follows. In Section 2, we present an equivalent formulation of the Landau-Lifshitz equation and some preliminaries needed in the sequel. In Section 3, we construct a class of length preserving IMEX-GSAV schemes, and derive an unconditional bound for the numerical solution. In Section 4, we carry out a rigorous error analysis for the new schemes up to fifth-order in a unified framework. In Section 5, we carry out a rigorous error analysis for the case where the nonlinear term is treated semi-implicitly. We present some numerical experiments in Section 6 to validate our theoretical results, and conclude with a few remarks in Section 7. In addition, we give error estimates for the auxiliary variable in Appendix A.

2. Reformulations for the Landau-Lifshitz equation and preliminaries

In this section, we first present an equivalent formulation of the Landau-Lifshitz equation, and then describe some notations and results which will be frequently used in this paper.

The Landau-Lifshitz Eq. (1.1) has several equivalent forms. Since it is very difficult to deal with the nonlinear term $\mathbf{m} \times (\mathbf{m} \times \Delta\mathbf{m})$ implicitly while an explicit treatment will lead to a severe time step constraint, we first rewrite the Landau-Lifshitz Eq. (1.1) as

$$\frac{\partial \mathbf{m}}{\partial t} = -\beta \mathbf{m} \times \Delta\mathbf{m} + \gamma \Delta\mathbf{m} + \gamma |\nabla \mathbf{m}|^2 \mathbf{m}, \quad \text{in } \Omega \times J, \tag{2.1}$$

by using $|\mathbf{m}| = 1$ and the identity

$$\mathbf{a} \times (\mathbf{b} \times \mathbf{c}) = (\mathbf{a} \cdot \mathbf{c})\mathbf{b} - (\mathbf{a} \cdot \mathbf{b})\mathbf{c}, \quad \mathbf{a}, \mathbf{b}, \mathbf{c} \in \mathbb{R}^3. \tag{2.2}$$

A case of particular interest is when $\beta = 0$, which leads to

$$\frac{\partial \mathbf{m}}{\partial t} = \gamma \Delta\mathbf{m} + \gamma |\nabla. \tag{2.3}$$

The above equation is also referred to as the heat flow for harmonic maps, and has been well studied (cf. [13,26]).

We now describe some notations and results which will be frequently used in this paper. Throughout the paper, we use C, with or without subscript, to denote a positive constant, which could have different values at different appearances.

We use the standard notations $L^2(\Omega)$, $H^k(\Omega)$ and $W^{k,p}(\Omega)$ to denote the usual Sobolev spaces over Ω. The norm corresponding to $H^k(\Omega)$ will be denoted simply by $\|\cdot\|_k$. In particular, $\|\cdot\|$ and $(\cdot,\cdot)$ are used to denote the norm and the inner product in $L^2(\Omega)$, respectively. The vectors and vector spaces will be indicated by boldface type.

The following lemmas will be frequently used in the sequel:

Lemma 1. *(Hölder inequality) Let $p, q, s > 0$ such that $\frac{1}{p} + \frac{1}{q} + \frac{1}{s} = 1$. Then for vector functions $\boldsymbol{u} \in \boldsymbol{L}^p(\Omega)$, $\boldsymbol{v} \in \boldsymbol{L}^q(\Omega)$, and scalar function $w \in L^s(\Omega)$, we have*

$$\int_\Omega |(\boldsymbol{u}, \boldsymbol{v}) w| d\boldsymbol{x} \le \|\boldsymbol{u}\|_{\boldsymbol{L}^p} \|\boldsymbol{v}\|_{\boldsymbol{L}^q} \|w\|_{L^s}. \tag{2.4}$$

Lemma 2. *(Interpolation inequalities) For any $\boldsymbol{f} \in \boldsymbol{H}^2(\Omega)$, then there exists a positive constant C such that*

$$\|\boldsymbol{f}\|_{\boldsymbol{L}^k} \le C \|\boldsymbol{f}\|_{\boldsymbol{L}^2}^{\frac{6-k}{2k}} \|\boldsymbol{f}\|_{\boldsymbol{H}^1}^{\frac{3k-6}{2k}}, \quad 3 \le k \le 6, \tag{2.5}$$

and

$$\|\boldsymbol{f}\|_{\boldsymbol{L}^\infty} \le C \|\boldsymbol{f}\|_{\boldsymbol{H}^1}^{\frac{1}{2}} \|\boldsymbol{f}\|_{\boldsymbol{H}^2}^{\frac{1}{2}}. \tag{2.6}$$

We will frequently use the following discrete version of the Gronwall lemma (see, for instance, [27,28]):

Lemma 3. *Let a_k, b_k, c_k, d_k, γ_k, Δt_k be non negative real numbers such that*

$$a_{k+1} - a_k + b_{k+1}\Delta t_{k+1} + c_{k+1}\Delta t_{k+1} - c_k \Delta t_k \le a_k d_k \Delta t_k + \gamma_{k+1}\Delta t_{k+1} \tag{2.7}$$

for all $0 \le k \le m$. Then

$$a_{m+1} + \sum_{k=0}^{m+1} b_k \Delta t_k \le \exp\left(\sum_{k=0}^{m} d_k \Delta t_k\right)\{a_0 + (b_0 + c_0)\Delta t_0 + \sum_{k=1}^{m+1} \gamma_k \Delta t_k\}. \tag{2.8}$$

3. Norm preserving and energy decreasing IMEX-GSAV schemes

We construct in this section higher-order norm preserving and energy decreasing schemes for the Landau-Lifshitz Eq. (2.1) based on the IMEX BDF-l formulae.

Set

$$\Delta t = T/N, \; t^n = n\Delta t, \; \text{for } n \le N,$$

and introduce an SAV

$$R(t) = E(\mathbf{m}) + K_0, \;\; E(\mathbf{m}) = \frac{1}{2}\|\nabla \mathbf{m}\|^2, \tag{3.1}$$

where K_0 is a positive constant. We expand the governing system as follows:

$$\frac{\partial \mathbf{m}}{\partial t} = \gamma \Delta\mathbf{m} + \gamma |\nabla \mathbf{m}|^2 \mathbf{m} - \beta \mathbf{m} \times \Delta\mathbf{m}, \tag{3.2}$$

$$\frac{dR}{dt} = -\frac{R}{E(\mathbf{m}) + K_0}\gamma \|\mathbf{m} \times \Delta\mathbf{m}\|^2, \tag{3.3}$$

$$|\mathbf{m}(\mathbf{x}, t)| = 1 \quad \forall \mathbf{x},\, t. \tag{3.4}$$

It is clear that, with $R(0) = E(\mathbf{m})|_{t=0} + K_0$, the solution of the original system (2.3) is also a solution of the above system. We construct below IMEX GSAV schemes for the expanded system (3.2)-(3.4).

Assuming $\mathbf{m}^j$, $\tilde{\mathbf{m}}^j$ with $j = n, n-1, \ldots, n-l+1$ are given, we solve $\tilde{\mathbf{m}}^{n+1}$ from

$$\begin{aligned} D_l\tilde{\mathbf{m}}^{n+1} =&\gamma\Delta\tilde{\mathbf{m}}^{n+1} + S\Delta(\tilde{\mathbf{m}}^{n+1} - B_l(\mathbf{m}^n)) \\ &+ \gamma|\nabla B_l(\mathbf{m}^n)|^2 B_l(\mathbf{m}^n) - \beta B_l(\mathbf{m}^n)\times\Delta B_l(\tilde{\mathbf{m}}^n), \end{aligned} \tag{3.5}$$

where $S \geq 0$ is a stabilization parameter, one can refer to [29,30] for further details. D_l denotes the BDF-l formula, and B_l is the l-th order Adams-Bashforth extrapolation operator. We note that the stabilization term is introduced to reduce the stability constraint caused by the explicit treatment of $\beta\mathbf{m}\times\Delta\mathbf{m}$.

Next we compute R^{n+1}, ξ^{n+1} from

$$\frac{R^{n+1} - R^n}{\Delta t} = -\gamma\xi^{n+1}\|B_l(\mathbf{m}^n)\times\Delta\tilde{\mathbf{m}}^{n+1}\|^2, \quad \xi^{n+1} = \frac{R^{n+1}}{E(\tilde{\mathbf{m}}^{n+1}) + K_0}, \tag{3.6}$$

where $R(t^{n+1}) = E(\mathbf{m}(t^{n+1})) + K_0$ and $E(\mathbf{m}(t^{n+1})) = \frac{1}{2}\int_\Omega |\nabla\mathbf{m}(t^{n+1})|^2\, d\mathbf{x}$.

Finally we update $\mathbf{m}^{n+1}$ by

$$\mathbf{m}^{n+1} = \frac{\hat{\mathbf{m}}^{n+1}}{|\hat{\mathbf{m}}^{n+1}|}, \text{ with } \hat{\mathbf{m}}^{n+1} = \eta_l^{n+1}\tilde{\mathbf{m}}^{n+1} + (1-\eta_l^{n+1})B_l(\tilde{\mathbf{m}}^n), \tag{3.7}$$

and

$$\eta_1^{n+1} = 1 - (1-\xi^{n+1})^2; \; \eta_l^{n+1} = 1 - (1-\xi^{n+1})^l, \; l \geq 2. \tag{3.8}$$

For readers' convenience, D_l and B_l with $l = 1, 2, 3$ are given below. Formulae for other l can be easily derived from Taylor expansions:

first-order scheme:

$$D_1\tilde{\mathbf{m}}^{n+1} = \frac{\tilde{\mathbf{m}}^{n+1} - \tilde{\mathbf{m}}^n}{\Delta t}, \; B_1(\mathbf{m}^n) = \mathbf{m}^n; \tag{3.9}$$

second-order scheme:

$$D_2\tilde{\mathbf{m}}^{n+1} = \frac{3\tilde{\mathbf{m}}^{n+1} - 4\tilde{\mathbf{m}}^n + \tilde{\mathbf{m}}^{n-1}}{2\Delta t}, \; B_2(\mathbf{m}^n) = 2\mathbf{m}^n - \mathbf{m}^{n-1}; \tag{3.10}$$

third-order scheme:

$$D_3\tilde{\mathbf{m}}^{n+1} = \frac{11\tilde{\mathbf{m}}^{n+1} - 18\tilde{\mathbf{m}}^n + 9\tilde{\mathbf{m}}^{n-1} - 2\tilde{\mathbf{m}}^{n-2}}{6\Delta t}, \; B_3(\mathbf{m}^n) = 3\mathbf{m}^n - 3\mathbf{m}^{n-1} + \mathbf{m}^{n-2}. \tag{3.11}$$

It is clear that the above scheme admits a unique solution, and it is very easy to implement as it only requires solving a vector Poisson type equation in (3.5).

Remark 1. In this work we only consider the time discretization. Note that the proposed IMEX GSAV schemes (3.5)-(3.8) can be easily implemented with finite difference and spectral methods, but theirs implementation with finite element methods needs special consideration when $\beta \neq 0$ due the explicit treatment for the term $\beta B_l(\mathbf{m}^n)\times\Delta B_l(\tilde{\mathbf{m}}^n)$. An additional, well-known difficulty in the case of finite element methods is that the normalization of a non-constant polynomial vector field is not polynomial. One can combine (3.5)-(3.8) with the Gauss-Seidel technique in [31] to treat the term $\beta B_l(\mathbf{m}^n)\times\Delta B_l(\tilde{\mathbf{m}}^n)$ semi-implicitly when the parameter β is relatively large.

Theorem 1. *Let $\{\boldsymbol{m}^n, \tilde{\boldsymbol{m}}^n, \hat{\boldsymbol{m}}^n\}$ be the solution of (3.5)-(3.8). Given $R^n > 0$, we have $\xi^{n+1} > 0$ and*

$$0 < R^{n+1} < R^n, \quad \forall n \leq T/\Delta t. \tag{3.12}$$

In addition, there exists a constant M_T independent of Δt such that

$$\|\nabla\hat{\boldsymbol{m}}^{n+1}\| + \sum_{k=0}^{n}\Delta t\gamma\xi^{k+1}\|B_l(\boldsymbol{m}^k)\times\Delta\tilde{\boldsymbol{m}}^{k+1}\|^2 \leq M_T, \quad \forall n \leq T/\Delta t, \text{and } n = l-1, \cdots, N-1. \tag{3.13}$$

Proof. Given $R^n > 0$, it follows from (3.6) that

$$R^{n+1} = \frac{1}{1 + \Delta t\gamma\frac{\|B_l(\mathbf{m}^n)\times\Delta\tilde{\mathbf{m}}^{n+1}\|^2}{E(\tilde{\mathbf{m}}^{n+1})+K_0}}R^n > 0. \tag{3.14}$$

In addition, multiplying (3.6) with Δt and taking the sum for n from 0 to m result in

$$R^{m+1} + \sum_{n=0}^{m}\Delta t\gamma\xi^{n+1}\|B_l(\mathbf{m}^n)\times\Delta\tilde{\mathbf{m}}^{n+1}\|^2 = R^0. \tag{3.15}$$

Denote $M := R^0$, then (3.15) implies

$$R^{m+1} + \sum_{n=0}^{m}\Delta t\gamma\xi^{n+1}\|B_l(\mathbf{m}^n)\times\Delta\tilde{\mathbf{m}}^{n+1}\|^2 \leq M. \tag{3.16}$$

It then follows from (3.6) that

$$\xi^{n+1}=\frac{R^{n+1}}{E(\tilde{\mathbf{m}}^{n+1})+K_0}\le\frac{2M}{\|\nabla\tilde{\mathbf{m}}^{n+1}\|^2+1},\tag{3.17}$$

where, without loss of generality, we assume that the positive constant $K_0\ge\frac{1}{2}$. We derive from (3.8) that $\eta_l^{n+1}=\xi^{n+1}P_q(\xi^{n+1})$, where P_q is a polynomial function of degree q with $q=1$ for $l=1$ and $q=l-1$ for $l>1$. We can then derive from (3.17) that there exists a positive constant M_1 such that

$$|\eta_l^{n+1}|=|\xi^{n+1}P_q(\xi^{n+1})|\le\frac{M_1}{\|\nabla\tilde{\mathbf{m}}^{n+1}\|^2+1}.\tag{3.18}$$

Thus we have

$$\|\nabla\hat{\mathbf{m}}^{n+1}\|^2=(\eta_l^{n+1})^2\|\nabla\tilde{\mathbf{m}}^{n+1}\|^2\le\left(\frac{M_1}{\|\nabla\tilde{\mathbf{m}}^{n+1}\|^2+1}\right)^2\|\nabla\tilde{\mathbf{m}}^{n+1}\|^2\le M_1^2,\tag{3.19}$$

which implies the desired results (3.13). □

Remark 2. The bound for $B_l(\mathbf{m}^k)\times\Delta\tilde{\mathbf{m}}^{k+1}$ in (3.13) is particularly useful in the error analysis.

4. Error estimate

In this section, we carry out a rigorous error analysis for (3.5)-(3.8).

We denote

$$\begin{aligned}\tilde{e}_{\mathbf{m}}^{n+1}=\mathbf{m}(t^{n+1})-\tilde{\mathbf{m}}^{n+1},\quad e_{\mathbf{m}}^{n+1}&=\mathbf{m}(t^{n+1})-\mathbf{m}^{n+1},\\ e_R^{n+1}&=R(t^{n+1})-R^{n+1}.\end{aligned}\tag{4.1}$$

We first recall the following important result by Nevanlinna and Odeh [32] based on Dahlquist's G-stability theory.

Lemma 4. *[32] For $1\le l\le 5$, there exists $0\le\tau_l<1$, a positive definite symmetric matrix $G=(g_{i,j})\in\mathbb{R}^{l,l}$, and real numbers $\theta_0,\dots,\theta_l$ such that*

$$\begin{aligned}\Delta t(D_l\boldsymbol{m}^{n+1},\boldsymbol{m}^{n+1}-\tau_l\boldsymbol{m}^n)=&\sum_{i,j=1}^{l}g_{i,j}(\boldsymbol{m}^{n+1+i-l},\boldsymbol{m}^{n+1+j-l})\\&-\sum_{i,j=1}^{l}g_{i,j}(\boldsymbol{m}^{n+i-l},\boldsymbol{m}^{n+j-l})+\|\sum_{i=0}^{l}\theta_i\boldsymbol{m}^{n+1+i-l}\|^2,\end{aligned}\tag{4.2}$$

where the smallest possible values of τ_l are

$$\tau_1=\tau_2=0,\ \tau_3=0.0836,\ \tau_4=0.2878,\ \tau_5=0.8160.$$

The proof of the following main result relies essentially on the stability result in (3.13) and the above lemma.

Theorem 2. *Supposing that the damping parameter γ satisfies*

$$\gamma>\frac{(|\beta|+S)(1+\tau_l)\sum_{i=0}^{l-1}|b_{l,i+1}|-S(1-\tau_l+b_{l,1}\tau_l)}{1-\tau_l},\tag{4.3}$$

and assuming $\boldsymbol{m}\in H^{l+1}(0,T;\boldsymbol{L}^2(\Omega))\bigcap H^l(0,T;\boldsymbol{W}^{1,3}(\Omega))\bigcap L^\infty(0,T;H^4(\Omega))$, then for the scheme (3.5)-(3.8), we have

$$\begin{aligned}&\|\boldsymbol{m}^{n+1}-\boldsymbol{m}(t^{n+1})\|^2+\|\nabla(\boldsymbol{m}^{n+1}-\boldsymbol{m}(t^{n+1}))\|^2+\|\hat{\boldsymbol{m}}^{n+1}-\boldsymbol{m}(t^{n+1})\|^2\\&+\|\nabla(\hat{\boldsymbol{m}}^{n+1}-\boldsymbol{m}(t^{n+1}))\|^2+\|\tilde{\boldsymbol{m}}^{n+1}-\boldsymbol{m}(t^{n+1})\|^2\\&+\|\nabla(\tilde{\boldsymbol{m}}^{n+1}-\boldsymbol{m}(t^{n+1}))\|^2+\Delta t\sum_{k=0}^{n}\|\Delta(\tilde{\boldsymbol{m}}^{k+1}-\boldsymbol{m}(t^{k+1}))\|^2\\\le&C(\Delta t)^{2l},\quad\forall\,0\le n\le N-1,\quad 1\le l\le 5,\end{aligned}$$

where $b_{l,j}$ denotes the coefficient of the j-th element for the operator B_l in (3.9)-(3.11) with $l=1,2,3$ and formulae for $l=4,5$ can be easily derived from Taylor expansions, and C is a positive constant independent of Δt.

Proof. We shall first prove, by an induction process with a bootstrap argument, that there exists a positive constant C_0 such that

$$|1-\xi^k|\le C_0\Delta t,\ \forall k\le T/\Delta t,\tag{4.4}$$

$$\|\tilde{e}_{\mathbf{m}}^k\|_{H^2}\le(\Delta t)^{1/4},\ \forall k\le T/\Delta t.\tag{4.5}$$

Obviously (4.4) and (4.5) hold for $k = 0$. Now we suppose

$$|1 - \xi^k| \le C_0 \Delta t, \ \forall k \le n, \tag{4.6}$$

$$\|\tilde{e}^k_{\mathbf{m}}\|_{H^2} \le (\Delta t)^{1/4}, \ \forall k \le n, \tag{4.7}$$

and prove below that $|1 - \xi^{n+1}| \le C_0 \Delta t$ and $\|\tilde{e}^{n+1}_{\mathbf{m}}\|_{H^2} \le (\Delta t)^{1/4}$ hold true. We shall carry out the induction proof in three steps below.
Step 1: A H^2 bound for $\tilde{e}^{n+1}_{\mathbf{m}}$. Following a similar procedure as in [33] and recalling the inequality

$$(a+b)^l \le 2^{l-1}(a^l + b^l), \ \forall a, b > 0, l \ge 1, \tag{4.8}$$

we can easily obtain from the induction assumption that under the condition $\Delta t \le \min\{\frac{1}{2^{l+2} C_0^l}, 1\}$, we have

$$\frac{1}{2} \le |\xi^k|, \ |\eta^k_l| \le 2, \quad \forall k \le n. \tag{4.9}$$

We first derive a useful relation between the error functions $e^k_{\mathbf{m}}$, $\hat{e}^k_{\mathbf{m}}$ and $\tilde{e}^k_{\mathbf{m}}$ in order to bound the nonlinear terms in the following analysis.

Lemma 5. *Assuming that (4.6) and (4.7) hold for all $1 \le k \le n$, $2 \le p \le 4$ and $1 \le l \le 5$, then we have*

$$\|e^k_{\boldsymbol{m}}\|_{W^{1,p}} \le C\|\hat{e}^k_{\boldsymbol{m}}\|_{W^{1,p}} \le C\|\tilde{e}^k_{\boldsymbol{m}}\|_{W^{1,p}} + C(C_0\Delta t)^q, \quad 1 \le k \le n, \tag{4.10}$$

where C is a positive constant independent of Δt and C_0, and $q = 2$ when $l = 1$, and $q = l$ when $l = 2, 3, 4, 5$ respectively.

Proof. Assuming that (4.7) holds for all $1 \le k \le n$, we have

$$\|\tilde{e}^k_{\mathbf{m}}\|_{L^\infty} \le C\|\tilde{e}^k_{\mathbf{m}}\|^{1/2}_{H^1}\|\tilde{e}^k_{\mathbf{m}}\|^{1/2}_{H^2} \le \frac{1}{8}, \tag{4.11}$$

under the condition $\Delta t \le (\frac{1}{8C_1})^4$. By using (3.8), (4.6) and (4.7), we have

$$\begin{aligned}
\|\hat{e}^k_{\mathbf{m}}\|_{L^\infty} \le& \|\mathbf{m}(t^k) - \tilde{\mathbf{m}}^k\|_{L^\infty} + \|\tilde{\mathbf{m}}^k - \hat{\mathbf{m}}^k\|_{L^\infty} \le \|\tilde{e}^k_{\mathbf{m}}\|_{L^\infty} + |1 - \eta^k_l|(\|\tilde{\mathbf{m}}^k\|_{L^\infty} + \|B_l(\tilde{\mathbf{m}}^{k-1})\|_{L^\infty}) \\
\le& \|\tilde{e}^k_{\mathbf{m}}\|_{L^\infty} + |1 - \xi^k|^q(\|\tilde{\mathbf{m}}^k\|_{L^\infty} + \|B_l(\tilde{\mathbf{m}}^{k-1})\|_{L^\infty}) \\
\le& \frac{1}{8} + (\|\tilde{\mathbf{m}}^k\|_{L^\infty} + \|B_l(\tilde{\mathbf{m}}^{k-1})\|_{L^\infty})(C_0\Delta t)^q \le \frac{1}{4},
\end{aligned} \tag{4.12}$$

where $\Delta t \le \frac{1}{17^{1/q} C_0}$. Here $q = 2$ when $l = 1$, and $q = l$ when $l = 2, 3, 4, 5$. Then for point-wise in Ω, we have

$$\frac{1}{2} \le |\hat{\mathbf{m}}^k| \le \frac{3}{2}. \tag{4.13}$$

By using exactly the same procedure as [12,13], there holds

$$\left|\frac{f}{|f|} - \frac{g}{|g|}\right| = \left|\frac{f(|g| - |f|) - |f|(g - f)}{|f||g|}\right| \le 2\frac{|f - g|}{|g|} \le C|f - g|, \tag{4.14}$$

where the constant C depends on $|g|$, and similarly we have

$$\left|\nabla \frac{f}{|f|} - \nabla \frac{g}{|g|}\right| \le C|\nabla g||f - g| + C|\nabla(f - g)|. \tag{4.15}$$

Thus we have

$$\|e^k_{\mathbf{m}}\|_{W^{1,p}} = \|\mathbf{m}(t^k) - \mathbf{m}^k\|_{W^{1,p}} = \left\|\frac{\mathbf{m}(t^k)}{|\mathbf{m}(t^k)|} - \frac{\hat{\mathbf{m}}^k}{|\hat{\mathbf{m}}^k|}\right\|_{W^{1,p}} \le C\|\hat{e}^k_{\mathbf{m}}\|_{W^{1,p}}. \tag{4.16}$$

Similarly as (4.12) and using (4.7), we can obtain

$$\begin{aligned}
\|\hat{e}^k_{\mathbf{m}}\|_{W^{1,p}} \le& \|\mathbf{m}(t^k) - \tilde{\mathbf{m}}^k\|_{W^{1,p}} + \|\tilde{\mathbf{m}}^k - \hat{\mathbf{m}}^k\|_{W^{1,p}} \\
\le& \|\tilde{e}^k_{\mathbf{m}}\|_{W^{1,p}} + |1 - \eta^k_l|(\|\tilde{\mathbf{m}}^k\|_{W^{1,p}} + \|B_l(\tilde{\mathbf{m}}^{k-1})\|_{W^{1,p}}) \\
\le& \|\tilde{e}^k_{\mathbf{m}}\|_{W^{1,p}} + |1 - \xi^k|^q(\|\tilde{\mathbf{m}}^k\|_{W^{1,p}} + \|B_l(\tilde{\mathbf{m}}^{k-1})\|_{W^{1,p}}) \\
\le& \|\tilde{e}^k_{\mathbf{m}}\|_{W^{1,p}} + C(C_0\Delta t)^q.
\end{aligned}$$

The proof is complete. □

We now continue with the proof of Theorem 2. Let $\mathbf{R}^{n+1}_{\mathbf{m},l}$ be the truncation error defined by

$$\mathbf{R}^{k+1}_{\mathbf{m},l} = \frac{\partial \mathbf{m}(t^{k+1})}{\partial t} - D_l \mathbf{m}(t^{k+1}) = \frac{1}{\Delta t}\sum_{i=1}^{l} \delta_i \int_{t^{k+1-i}}^{t^{k+1}} (t^{k+1-i} - t)^l \frac{\partial^{l+1}\mathbf{m}}{\partial t^{l+1}} dt, \tag{4.17}$$

with δ_i being some fixed and bounded constants. Subtracting (3.5) from (3.2) at t^{k+1}, we obtain an error equation corresponding to (3.5):

$$\begin{aligned} D_l\tilde{e}_{\mathbf{m}}^{k+1}-\gamma\Delta\tilde{e}_{\mathbf{m}}^{k+1}=&-\gamma\big(|\nabla B_l(\mathbf{m}^k)|^2B_l(\mathbf{m}^k)-|\nabla\mathbf{m}(t^{k+1})|^2\mathbf{m}(t^{k+1})\big)-\mathbf{R}_{\mathbf{m},l}^{k+1}\\ &-\beta\big(\mathbf{m}(t^{k+1})\times\Delta\mathbf{m}(t^{k+1})-B_l(\mathbf{m}^k)\times\Delta B_l(\tilde{\mathbf{m}}^k)\big)\\ &+S\big((\Delta\tilde{e}_{\mathbf{m}}^{k+1}-\Delta B_l(\tilde{e}_{\mathbf{m}}^k))-(\Delta\mathbf{m}(t^{k+1})-\Delta B_l(\mathbf{m}(t^k)))\big). \end{aligned} \tag{4.18}$$

Taking the inner product of (4.18) with $-\Delta t(\Delta\tilde{e}_{\mathbf{m}}^{k+1}-\tau_l\Delta\tilde{e}_{\mathbf{m}}^k)$ and using Lemma 4, we obtain

$$\begin{aligned} &\sum_{i,j=1}^{l}g_{i,j}(\nabla\tilde{e}_{\mathbf{m}}^{k+1+i-l},\nabla\tilde{e}_{\mathbf{m}}^{k+1+j-l})-\sum_{i,j=1}^{l}g_{i,j}(\nabla\tilde{e}_{\mathbf{m}}^{k+i-l},\nabla\tilde{e}_{\mathbf{m}}^{k+j-l})\\ &+\|\sum_{i=0}^{l}\theta_i\nabla\tilde{e}_{\mathbf{m}}^{k+1+i-l}\|^2+\Delta t\gamma\|\Delta\tilde{e}_{\mathbf{m}}^{k+1}\|^2 \\ =&\Delta t\gamma\big(|\nabla B_l(\mathbf{m}^k)|^2-|\nabla B_l(\mathbf{m}(t^k))|^2,B_l(\mathbf{m}^k)(\Delta\tilde{e}_{\mathbf{m}}^{k+1}-\tau_l\Delta\tilde{e}_{\mathbf{m}}^k)\big)\\ &-\Delta t\gamma\big(|\nabla B_l(\mathbf{m}(t^k))|^2B_l(e_{\mathbf{m}}^k),\Delta\tilde{e}_{\mathbf{m}}^{k+1}-\tau_l\Delta\tilde{e}_{\mathbf{m}}^k\big)\\ &+\Delta t\gamma\big(|\nabla B_l(\mathbf{m}(t^k))|^2B_l(\mathbf{m}(t^k))-|\nabla\mathbf{m}(t^{k+1})|^2\mathbf{m}(t^{k+1}),\Delta\tilde{e}_{\mathbf{m}}^{k+1}-\tau_l\Delta\tilde{e}_{\mathbf{m}}^k)\big)\\ &+\Delta t\gamma(\Delta\tilde{e}_{\mathbf{m}}^{k+1},\tau_l\Delta\tilde{e}_{\mathbf{m}}^k)+\Delta t(\mathbf{R}_{\mathbf{m},l}^{k+1},\Delta\tilde{e}_{\mathbf{m}}^{k+1}-\tau_l\Delta\tilde{e}_{\mathbf{m}}^k))\\ &+\Delta t\beta\big(\big(\mathbf{m}(t^{k+1})\times\Delta\mathbf{m}(t^{k+1})-B_l(\mathbf{m}^k)\times\Delta B_l(\tilde{\mathbf{m}}^k)\big),\Delta\tilde{e}_{\mathbf{m}}^{k+1}-\tau_l\Delta\tilde{e}_{\mathbf{m}}^k\big)\\ &-S\Delta t\big((\Delta\tilde{e}_{\mathbf{m}}^{k+1}-\Delta B_l(\tilde{e}_{\mathbf{m}}^k))-(\Delta\mathbf{m}(t^{k+1})-\Delta B_l(\mathbf{m}(t^k))),\Delta\tilde{e}_{\mathbf{m}}^{k+1}-\tau_l\Delta\tilde{e}_{\mathbf{m}}^k\big)\\ =&\Delta t(I_1+I_2+I_3+I_4+I_5+I_6+I_7). \end{aligned} \tag{4.19}$$

We bound the above seven terms as follows. Using the Hölder inequality in Lemma 1 and Lemma 5, and applying the interpolation inequality (2.5), (4.7) and Cauchy-Schwarz inequality, we have

$$\begin{aligned} |I_1|=&\gamma\big(|\nabla B_l(\mathbf{m}^k)|^2-|\nabla B_l(\mathbf{m}(t^k))|^2,B_l(\mathbf{m}^k)(\Delta\tilde{e}_{\mathbf{m}}^{k+1}-\tau_l\Delta\tilde{e}_{\mathbf{m}}^k)\big)\\ \le&C(\Delta t)^{1/4}\|\nabla B_l(\tilde{e}_{\mathbf{m}}^k)\|_{L^2}^{1/2}\|\Delta B_l(\tilde{e}_{\mathbf{m}}^k)\|_{L^2}^{1/2}\|B_l(\mathbf{m}^k)(\Delta\tilde{e}_{\mathbf{m}}^{k+1}-\tau_l\Delta\tilde{e}_{\mathbf{m}}^k)\|_{L^2}\\ &+C\|\nabla B_l(\mathbf{m}(t^k))\|_{L^6}\|\nabla B_l(\tilde{e}_{\mathbf{m}}^k)\|_{L^2}^{1/2}\|\Delta B_l(\tilde{e}_{\mathbf{m}}^k)\|_{L^2}^{1/2}\|B_l(\mathbf{m}^k)(\Delta\tilde{e}_{\mathbf{m}}^{k+1}-\tau_l\Delta\tilde{e}_{\mathbf{m}}^k)\|_{L^2}\\ &+C(C_0\Delta t)^q((C_0\Delta t)^q+\|\nabla B_l(\mathbf{m}(t^k))\|_{L^6}+\|\nabla B_l(\tilde{e}_{\mathbf{m}}^k))\|B_l(\mathbf{m}^k)(\Delta\tilde{e}_{\mathbf{m}}^{k+1}-\tau_l\Delta\tilde{e}_{\mathbf{m}}^k)\|_{L^2}\\ \le&\epsilon\|\Delta\tilde{e}_{\mathbf{m}}^{k+1}\|_{L^2}^2+\frac{\epsilon}{l}\sum_{i=0}^{l-1}\|\Delta\tilde{e}_{\mathbf{m}}^{k-i}\|_{L^2}^2+C\|\nabla B_l(\tilde{e}_{\mathbf{m}}^k)\|_{L^2}^2+C(C_0\Delta t)^{2q}, \end{aligned} \tag{4.20}$$

where ϵ is an arbitrarily small positive constant which is independent of Δt and will be determined below. Using the Hölder inequality in Lemma 1 , the second term on the right-hand side of (4.19) can be bounded by

$$\begin{aligned} |I_2|=&\gamma|\big(|\nabla B_l(\mathbf{m}(t^k))|^2B_l(e_{\mathbf{m}}^k),\Delta\tilde{e}_{\mathbf{m}}^{k+1}-\tau_l\Delta\tilde{e}_{\mathbf{m}}^k\big)|\\ \le&\gamma\|(\nabla B_l(\mathbf{m}(t^k)))^2\|_{L^3}\|B_l(e_{\mathbf{m}}^k)\|_{L^6}\|\Delta\tilde{e}_{\mathbf{m}}^{k+1}-\tau_l\Delta\tilde{e}_{\mathbf{m}}^k\|_{L^2}\\ \le&\gamma\|\nabla B_l(\mathbf{m}(t^k))\|_{L^6}^2\|B_l(e_{\mathbf{m}}^k)\|_{L^6}\|\Delta\tilde{e}_{\mathbf{m}}^{k+1}-\tau_l\Delta\tilde{e}_{\mathbf{m}}^k\|_{L^2}\\ \le&\epsilon\|\Delta\tilde{e}_{\mathbf{m}}^{k+1}\|_{L^2}^2+\epsilon\|\Delta\tilde{e}_{\mathbf{m}}^k\|_{L^2}^2+C\|\nabla B_l(\mathbf{m}(t^k))\|_{L^6}^4\|\nabla B_l(\tilde{e}_{\mathbf{m}}^k)\|_{L^2}^2. \end{aligned} \tag{4.21}$$

For the third term on the right-hand side of (4.19), we have

$$\begin{aligned} |I_3|=&\gamma\big(|\nabla B_l(\mathbf{m}(t^k))|^2B_l(\mathbf{m}(t^k))-|\nabla\mathbf{m}(t^{k+1})|^2\mathbf{m}(t^{k+1}),\Delta\tilde{e}_{\mathbf{m}}^{k+1}-\tau_l\Delta\tilde{e}_{\mathbf{m}}^k)\big)\\ =&\gamma\big(|\nabla B_l(\mathbf{m}(t^k))|^2(B_l(\mathbf{m}(t^k))-\mathbf{m}(t^{k+1})),\Delta\tilde{e}_{\mathbf{m}}^{k+1}-\tau_l\Delta\tilde{e}_{\mathbf{m}}^k)\big)\\ &+\gamma\big(|\nabla B_l(\mathbf{m}(t^k))|^2-|\nabla\mathbf{m}(t^{k+1})|^2,\mathbf{m}(t^{k+1})(\Delta\tilde{e}_{\mathbf{m}}^{k+1}-\tau_l\Delta\tilde{e}_{\mathbf{m}}^k)\big). \end{aligned} \tag{4.22}$$

Thus using the Hölder inequality, the above term can be bounded by

$$\begin{aligned} |I_3|\le&\epsilon\|\Delta\tilde{e}_{\mathbf{m}}^{k+1}\|_{L^2}^2+\epsilon\|\Delta\tilde{e}_{\mathbf{m}}^k\|_{L^2}^2+C\|\nabla B_l(\mathbf{m}(t^k))\|_{L^6}^2\|\sum_{i=1}^{l}d_i\int_{k+1-i}^{k+1}(t^{k+1-i}-s)^{l-1}\frac{\partial^l\mathbf{m}}{\partial t^l}(s)ds\|_{L^3}^2\\ &+C(\|\nabla B_l(\mathbf{m}(t^k))\|_{L^6}^2+\|\nabla\mathbf{m}(t^{k+1})\|_{L^6}^2)\|\sum_{i=1}^{l}d_i\int_{k+1-i}^{k+1}(t^{k+1-i}-s)^{l-1}\frac{\partial^l\nabla\mathbf{m}}{\partial t^l}(s)ds\|_{L^3}^2\\ \le&\epsilon\|\Delta\tilde{e}_{\mathbf{m}}^{k+1}\|_{L^2}^2+\epsilon\|\Delta\tilde{e}_{\mathbf{m}}^k\|_{L^2}^2+C(\Delta t)^{2l-1}\|\nabla\mathbf{m}(t^{k+1})\|_{L^6}^2\int_{k+1-l}^{k+1}\|\frac{\partial^l\mathbf{m}}{\partial t^l}(s)\|_{W^{1,3}}^2ds\\ &+C(\Delta t)^{2l-1}\|\nabla B_l(\mathbf{m}(t^k))\|_{L^6}^2\int_{k+1-l}^{k+1}\|\frac{\partial^l\mathbf{m}}{\partial t^l}(s)\|_{W^{1,3}}^2ds, \end{aligned} \tag{4.23}$$

where d_i with $i = 1, 2, \dots, 4, 5$ are some fixed and bounded constants determined by the truncation errors.

For the fourth term on the right hand side of (4.19), we have

$$|I_4| = \gamma|(\Delta\tilde{e}_{\mathbf{m}}^{k+1}, \tau_l\Delta\tilde{e}_{\mathbf{m}}^{k})| \le \frac{\gamma\tau_l}{2}\|\Delta\tilde{e}_{\mathbf{m}}^{k+1}\|_{L^2}^2 + \frac{\gamma\tau_l}{2}|\Delta\tilde{e}_{\mathbf{m}}^{k}\|_{L^2}^2. \tag{4.24}$$

Recalling (4.17), the fifth term on the right hand side of (4.19) can be controlled by

$$\begin{aligned}|I_5| =&|(\mathbf{R}_{\mathbf{m},l}^{k+1}, \Delta\tilde{e}_{\mathbf{m}}^{k+1} - \tau_l\Delta\tilde{e}_{\mathbf{m}}^{k}))|\\ \le&\epsilon\|\Delta\tilde{e}_{\mathbf{m}}^{k+1}\|_{L^2}^2 + \epsilon\|\Delta\tilde{e}_{\mathbf{m}}^{k}\|_{L^2}^2 + C(\Delta t)^{2l-1}\int_{k+1-l}^{k+1}\|\frac{\partial^{l+1}\mathbf{m}}{\partial t^{l+1}}(s)\|_{L^2}^2 ds.\end{aligned} \tag{4.25}$$

The sixth term on the right hand side of (4.19) can be estimated by

$$\begin{aligned}|I_6| =&|\beta|\Big|\big(\mathbf{m}(t^{k+1})\times\Delta\mathbf{m}(t^{k+1}) - B_l(\mathbf{m}^k)\times\Delta B_l(\tilde{\mathbf{m}}^k), \Delta\tilde{e}_{\mathbf{m}}^{k+1} - \tau_l\Delta\tilde{e}_{\mathbf{m}}^{k}\big)\Big|\\ =&|\beta|\Big|\big(\mathbf{m}(t^{k+1})\times(\Delta\mathbf{m}(t^{k+1}) - \Delta B_l(\mathbf{m}(t^k))), \Delta\tilde{e}_{\mathbf{m}}^{k+1} - \tau_l\Delta\tilde{e}_{\mathbf{m}}^{k}\big)\Big|\\ &+|\beta|\Big|\big(B_l(e_{\mathbf{m}}^k)\times\Delta B_l(\tilde{\mathbf{m}}^k), \Delta\tilde{e}_{\mathbf{m}}^{k+1} - \tau_l\Delta\tilde{e}_{\mathbf{m}}^{k}\big)\Big|\\ &+|\beta|\Big|\big(\mathbf{m}(t^{k+1})\times\Delta B_l(\tilde{e}_{\mathbf{m}}^k), \Delta\tilde{e}_{\mathbf{m}}^{k+1} - \tau_l\Delta\tilde{e}_{\mathbf{m}}^{k}\big)\Big|\\ &+|\beta|\Big|\big((\mathbf{m}(t^{k+1}) - B_l(\mathbf{m}(t^k)))\times\Delta B_l(\tilde{\mathbf{m}}^k), \Delta\tilde{e}_{\mathbf{m}}^{k+1} - \tau_l\Delta\tilde{e}_{\mathbf{m}}^{k}\big)\Big|.\end{aligned} \tag{4.26}$$

Applying Cauchy-Schwarz inequality, the first term on the right hand side of (4.26) can be estimated by

$$\begin{aligned}&|\beta|\Big|\big(\mathbf{m}(t^{k+1})\times(\Delta\mathbf{m}(t^{k+1}) - \Delta B_l(\mathbf{m}(t^k))), \Delta\tilde{e}_{\mathbf{m}}^{k+1} - \tau_l\Delta\tilde{e}_{\mathbf{m}}^{k}\big)\Big|\\ \le&|\beta|\|\sum_{i=1}^{l} d_i\int_{k+1-i}^{k+1}(t^{k+1-i} - s)^{l-1}\frac{\partial^l\Delta\mathbf{m}}{\partial t^l}(s)ds\|_{L^2}\|\mathbf{m}(t^{k+1})\|_{L^\infty}\|\Delta\tilde{e}_{\mathbf{m}}^{k+1} - \tau_l\Delta\tilde{e}_{\mathbf{m}}^{k}\|_{L^2}\\ \le&\epsilon\|\Delta\tilde{e}_{\mathbf{m}}^{k+1}\|_{L^2}^2 + \epsilon\|\Delta\tilde{e}_{\mathbf{m}}^{k}\|_{L^2}^2 + C(\Delta t)^{2l-1}\int_{k+1-l}^{k+1}\|\frac{\partial^l\mathbf{m}}{\partial t^l}(s)\|_{H^2}^2 ds.\end{aligned} \tag{4.27}$$

Applying the interpolation inequality (2.6), (3.7) and (4.7), the second term on the right hand side of (4.26) can be bounded by

$$\begin{aligned}&|\beta|\Big|\big(B_l(e_{\mathbf{m}}^k)\times\Delta B_l(\tilde{\mathbf{m}}^k), \Delta\tilde{e}_{\mathbf{m}}^{k+1} - \tau_l\Delta\tilde{e}_{\mathbf{m}}^{k}\big)\Big|\\ \le&\beta\|B_l(e_{\mathbf{m}}^k)\|_{L^\infty}\|\Delta B_l(\tilde{\mathbf{m}}^k)\|_{L^2}\|\Delta\tilde{e}_{\mathbf{m}}^{k+1} - \tau_l\Delta\tilde{e}_{\mathbf{m}}^{k}\|_{L^2}\\ \le&C|\beta|\|B_l(\tilde{e}_{\mathbf{m}}^k)\|_{H^1}^{1/2}\|B_l(\tilde{e}_{\mathbf{m}}^k)\|_{H^2}^{1/2}\|\Delta B_l(\tilde{\mathbf{m}}^k)\|_{L^2}\|\Delta\tilde{e}_{\mathbf{m}}^{k+1} - \tau_l\Delta\tilde{e}_{\mathbf{m}}^{k}\|_{L^2}\\ \le&\epsilon\|\Delta\tilde{e}_{\mathbf{m}}^{k+1}\|_{L^2}^2 + \frac{\epsilon}{l}\sum_{i=0}^{l-1}\|\Delta\tilde{e}_{\mathbf{m}}^{k-i}\|_{L^2}^2 + C\|\nabla B_l(\tilde{e}_{\mathbf{m}}^k)\|_{L^2}^2.\end{aligned} \tag{4.28}$$

Using Cauchy-Schwarz inequality, the third term on the right hand side of (4.26) can be bounded by

$$\begin{aligned}&|\beta|\Big|\big(\mathbf{m}(t^{k+1})\times\Delta B_l(\tilde{e}_{\mathbf{m}}^k), \Delta\tilde{e}_{\mathbf{m}}^{k+1} - \tau_l\Delta\tilde{e}_{\mathbf{m}}^{k}\big)\Big|\\ \le&|\beta|\|\mathbf{m}(t^{k+1})\|_{L^\infty}\|\Delta B_l(\tilde{e}_{\mathbf{m}}^k)\|_{L^2}(\|\Delta\tilde{e}_{\mathbf{m}}^{k+1}\| + \tau_l\|\Delta\tilde{e}_{\mathbf{m}}^{k}\|_{L^2})\\ \le&|\beta|\|\mathbf{m}(t^{k+1})\|_{L^\infty}\sum_{i=0}^{l-1}|b_{l,i+1}|\|\Delta\tilde{e}_{\mathbf{m}}^{k-i}\|_{L^2}(\|\Delta\tilde{e}_{\mathbf{m}}^{k+1}\| + \tau_l\|\Delta\tilde{e}_{\mathbf{m}}^{k}\|_{L^2})\\ \le&\frac{|\beta|(\tau_l+1)}{2}\sum_{i=0}^{l-1}|b_{l,i+1}|\|\Delta\tilde{e}_{\mathbf{m}}^{k-i}\|_{L^2}^2 + \frac{|\beta|}{2}(\sum_{i=0}^{l-1}|b_{l,i+1}|)\|\Delta\tilde{e}_{\mathbf{m}}^{k+1}\|_{L^2}^2 + \frac{|\beta|\tau_l}{2}(\sum_{i=0}^{l-1}|b_{l,i+1}|)\|\Delta\tilde{e}_{\mathbf{m}}^{k}\|_{L^2}^2,\end{aligned} \tag{4.29}$$

where $b_{l,j}$ denotes the coefficient of the j-th element for the operator B_l. Applying the interpolation inequality (2.6), (3.7) and (4.7), the last term on the right hand side of (4.26) can be estimated by

$$\begin{aligned}&|\beta|\Big|\big((\mathbf{m}(t^{k+1}) - B_l(\mathbf{m}(t^k)))\times\Delta B_l(\tilde{\mathbf{m}}^k), \Delta\tilde{e}_{\mathbf{m}}^{k+1} - \tau_l\Delta\tilde{e}_{\mathbf{m}}^{k}\big)\Big|\\ \le&|\beta|\|\sum_{i=1}^{l} d_i\int_{k+1-i}^{k+1}(t^{k+1-i} - s)^{l-1}\frac{\partial^l\mathbf{m}}{\partial t^l}(s)ds\|_{L^\infty}\|\Delta B_l(\tilde{\mathbf{m}}^k)\|_{L^2}\|\Delta\tilde{e}_{\mathbf{m}}^{k+1} - \tau_l\Delta\tilde{e}_{\mathbf{m}}^{k}\|_{L^2}\\ \le&\epsilon\|\Delta\tilde{e}_{\mathbf{m}}^{k+1}\|_{L^2}^2 + \epsilon\|\Delta\tilde{e}_{\mathbf{m}}^{k}\|_{L^2}^2 + C(\Delta t)^{2l-1}\int_{k+1-l}^{k+1}\|\frac{\partial^l\mathbf{m}}{\partial t^l}(s)\|_{H^2}^2 ds.\end{aligned} \tag{4.30}$$

Therefore, it remains to estimate the last term on the right hand side of (4.19). We have

$$\begin{aligned}I_7 =&-S\big((\Delta\tilde{e}_{\mathbf{m}}^{k+1} - \Delta B_l(\tilde{e}_{\mathbf{m}}^k)) - (\Delta\mathbf{m}(t^{k+1}) - \Delta B_l(\mathbf{m}(t^k))), \Delta\tilde{e}_{\mathbf{m}}^{k+1} - \tau_l\Delta\tilde{e}_{\mathbf{m}}^{k}\big)\\ =&-S(\|\Delta\tilde{e}_{\mathbf{m}}^{k+1}\|^2 + b_{l,1}\tau_l\|\Delta\tilde{e}_{\mathbf{m}}^{k}\|^2) + S(\Delta\tilde{e}_{\mathbf{m}}^{k+1}, \tau_l\Delta\tilde{e}_{\mathbf{m}}^{k})\end{aligned} \tag{4.31}$$

$$+ S(\sum_{i=1}^{l-1} b_{l,i+1}\Delta\tilde{e}_{\mathbf{m}}^{k-i}, \Delta\tilde{e}_{\mathbf{m}}^{k+1} - \tau_l\Delta\tilde{e}_{\mathbf{m}}^{k}) + S\big(\Delta\mathbf{m}(t^{k+1}) - \Delta B_l(\mathbf{m}(t^k)), \Delta\tilde{e}_{\mathbf{m}}^{k+1} - \tau_l\Delta\tilde{e}_{\mathbf{m}}^{k}\big).$$

The first term on the right hand side of (4.31) should be moved to the left hand of (4.19), thus we only need to estimate the second to fourth terms on the right hand of above equation, which can be controlled by

$$\begin{aligned}
S(\Delta\tilde{e}_{\mathbf{m}}^{k+1}, \tau_l\Delta\tilde{e}_{\mathbf{m}}^{k})+&S(\sum_{i=1}^{l-1} b_{l,i+1}\Delta\tilde{e}_{\mathbf{m}}^{k-i}, \Delta\tilde{e}_{\mathbf{m}}^{k+1} - \tau_l\Delta\tilde{e}_{\mathbf{m}}^{k})\\
&+ S\big(\Delta\mathbf{m}(t^{k+1}) - \Delta B_l(\mathbf{m}(t^k)), \Delta\tilde{e}_{\mathbf{m}}^{k+1} - \tau_l\Delta\tilde{e}_{\mathbf{m}}^{k}\big)\\
\le&\frac{S\tau_l}{2}\|\Delta\tilde{e}_{\mathbf{m}}^{k+1}\|^2 + \frac{S\tau_l}{2}\|\Delta\tilde{e}_{\mathbf{m}}^{k}\|^2 + \frac{S(\tau_l+1)}{2}\sum_{i=1}^{l-1}|b_{l,i+1}|\|\Delta\tilde{e}_{\mathbf{m}}^{k-i}\|_{L^2}^2\\
&+ \frac{S}{2}(\sum_{i=1}^{l-1}|b_{l,i+1}|)\|\Delta\tilde{e}_{\mathbf{m}}^{k+1}\|_{L^2}^2 + \frac{S\tau_l}{2}(\sum_{i=1}^{l-1}|b_{l,i+1}|)\|\Delta\tilde{e}_{\mathbf{m}}^{k}\|_{L^2}^2\\
&+ \epsilon\|\Delta\tilde{e}_{\mathbf{m}}^{k+1}\|_{L^2}^2 + \epsilon\|\Delta\tilde{e}_{\mathbf{m}}^{k}\|_{L^2}^2 + C(\Delta t)^{2l-1}\int_{k+1-l}^{k+1}\|\frac{\partial^l\mathbf{m}}{\partial t^l}(s)\|_{H^2}^2 ds.
\end{aligned} \tag{4.32}$$

Finally combining (4.19) with (4.20)-(4.32), we obtain

$$\begin{aligned}
&\sum_{i,j=1}^{l} g_{i,j}(\nabla\tilde{e}_{\mathbf{m}}^{k+1+i-l}, \nabla\tilde{e}_{\mathbf{m}}^{k+1+j-l}) - \sum_{i,j=1}^{l} g_{i,j}(\nabla\tilde{e}_{\mathbf{m}}^{k+i-l}, \nabla\tilde{e}_{\mathbf{m}}^{k+j-l})\\
&+ \|\sum_{i=0}^{l}\theta_i\nabla\tilde{e}_{\mathbf{m}}^{k+1+i-l}\|^2 + (S+\gamma)\Delta t\|\Delta\tilde{e}_{\mathbf{m}}^{k+1}\|^2 + Sb_{l,1}\tau_l\Delta t\|\Delta\tilde{e}_{\mathbf{m}}^{k}\|^2\\
\le&(8\epsilon + \frac{(\gamma+S)\tau_l}{2} + \frac{|\beta|+S}{2}\sum_{i=0}^{l-1}|b_{l,i+1}|)\Delta t\|\Delta\tilde{e}_{\mathbf{m}}^{k+1}\|_{L^2}^2\\
&+ (6\epsilon + \frac{(\gamma+S)\tau_l}{2} + \frac{(|\beta|+S)\tau_l}{2}\sum_{i=0}^{l-1}|b_{l,i+1}|)\Delta t\|\Delta\tilde{e}_{\mathbf{m}}^{k}\|_{L^2}^2\\
&+ \frac{2\epsilon}{l}\sum_{i=0}^{l-1}\Delta t\|\Delta\tilde{e}_{\mathbf{m}}^{k-i}\|_{L^2}^2 + \Delta t\frac{(|\beta|+S)(\tau_l+1)}{2}\sum_{i=0}^{l-1}|b_{l,i+1}|\|\Delta\tilde{e}_{\mathbf{m}}^{k-i}\|_{L^2}^2 + C\Delta t\|\nabla B_l(\tilde{e}_{\mathbf{m}}^{k})\|_{L^2}^2\\
&+ C\Delta t(C_0\Delta t)^{2q} + C\Delta t\|\nabla B_l(\mathbf{m}(t^k))\|_{L^6}^4\|\nabla B_l(\tilde{e}_{\mathbf{m}}^{k})\|_{L^2}^2\\
&+ C(\Delta t)^{2l}\int_{k+1-l}^{k+1}\left(\|\frac{\partial^l\mathbf{m}}{\partial t^l}(s)\|_{W^{1,3}}^2 + \|\frac{\partial^{l+1}\mathbf{m}}{\partial t^{l+1}}(s)\|_{L^2}^2 + \|\frac{\partial^l\mathbf{m}}{\partial t^l}(s)\|_{H^2}^2\right)ds,
\end{aligned} \tag{4.33}$$

where $q = 2$ with $l = 1$ and $q = l$ with $l = 2, 3, 4, 5$ respectively.

Summing (4.33) over k from 0 to n, and thanks to Lemma 4, $G = (g_{i,j})$ is a symmetric positive definite matrix with minimum eigenvalue $\lambda_{\min}$, we obtain

$$\begin{aligned}
&\frac{\lambda_{\min}}{l}\|\nabla\tilde{e}_{\mathbf{m}}^{n+1}\|^2 + \left((\gamma+S)(1-\tau_l) + Sb_{l,1}\tau_l - (|\beta|+S)(1+\tau_l)\sum_{i=0}^{l-1}|b_{l,i+1}| - 16\epsilon\right)\Delta t\sum_{k=0}^{n}\|\Delta\tilde{e}_{\mathbf{m}}^{k+1}\|^2\\
\le&C\sum_{k=0}^{n}\Delta t\|\nabla B_l(\tilde{e}_{\mathbf{m}}^{k})\|_{L^2}^2 + C(C_0\Delta t)^{2q} + C\sum_{k=0}^{n}\Delta t\|\nabla B_l(\mathbf{m}(t^k))\|_{L^6}^4\|\nabla B_l(\tilde{e}_{\mathbf{m}}^{k})\|_{L^2}^2\\
&+ C(\Delta t)^{2l}\int_0^T\|\frac{\partial^l\mathbf{m}}{\partial t^l}(s)\|_{W^{1,3}}^2 ds + C(\Delta t)^{2l}\int_0^T\|\frac{\partial^{l+1}\mathbf{m}}{\partial t^{l+1}}(s)\|_{L^2}^2 ds.
\end{aligned} \tag{4.34}$$

Using the condition (4.3) and setting

$$\epsilon = \frac{(\gamma+S)(1-\tau_l) + Sb_{l,1}\tau_l - (|\beta|+S)(1+\tau_l)\sum_{i=0}^{l-1}|b_{l,i+1}|}{32},$$

and applying the discrete Gronwall Lemma 3 to (4.34), we can arrive at

$$\|\nabla\tilde{e}_{\mathbf{m}}^{n+1}\|^2 + \Delta t\sum_{k=0}^{n}\|\Delta\tilde{e}_{\mathbf{m}}^{k+1}\|^2 \le \begin{cases} C_1\big(1 + C_0^4(\Delta t)^2\big)(\Delta t)^2, & l = 1,\\ C_1\big(1 + C_0^{2l}\big)(\Delta t)^{2l}, & l = 2,3,4,5, \end{cases} \tag{4.35}$$

where C_1 is independent of C_0 and Δt.

Thus taking the inner product of (4.18) with $\Delta t(\tilde{e}_{\mathbf{m}}^{k+1} - \tau_l\tilde{e}_{\mathbf{m}}^{k})$ and using the similar procedure as above, we can easily obtain that

$$\|\tilde{e}_{\mathbf{m}}^{n+1}\|^2 + \|\nabla\tilde{e}_{\mathbf{m}}^{n+1}\|^2 + \Delta t\sum_{k=0}^{n}\|\Delta\tilde{e}_{\mathbf{m}}^{k+1}\|^2 \le \begin{cases} C_2\big(1 + C_0^4(\Delta t)^2\big)(\Delta t)^2, & l = 1,\\ C_2\big(1 + C_0^{2l}\big)(\Delta t)^{2l}, & l = 2,3,4,5, \end{cases} \tag{4.36}$$

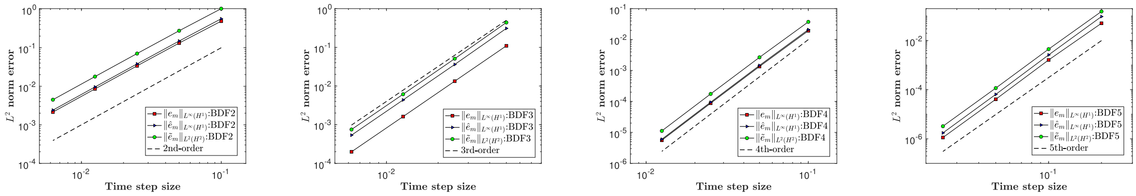

(a) BDF2 vs. errors (b) BDF3 vs. errors (c) BDF4 vs. errors (d) BDF5 vs. errors

Fig. 1. Convergence rates of the second- to fifth-order schemes based on BDF-l temporal stencil in (3.9)-(3.11) with $\beta = 0$ and $S = 0$ in Example 1. (For interpretation of the references to colour in this figure legend, the reader is referred to the web version of this article.)

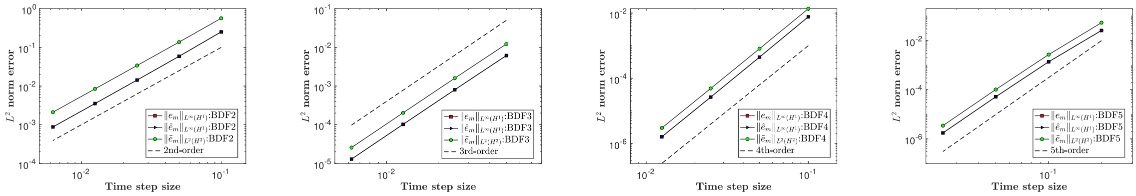

(a) BDF2 vs. errors (b) BDF3 vs. errors (c) BDF4 vs. errors (d) BDF5 vs. errors

Fig. 2. Convergence rates of the second- to fifth-order schemes based on BDF-l temporal stencil in (3.9)-(3.11) replaced by the original magnetization vector variables from previous time steps with $\beta = 0$ and $S = 0$ in Example 1. (For interpretation of the references to colour in this figure legend, the reader is referred to the web version of this article.)

where C_2 is independent of C_0 and Δt.

Step 2: Estimates for $|1-\xi^{n+1}|$. We shall first start by establishing an error equation corresponding to (3.6). The detailed proof of this section is provided in the appendix to save space. By using Lemma 6, we have

$$|e_R^{n+1}|^2 \le \begin{cases} C_4\big(1 + C_0^4(\Delta t)^2\big)(\Delta t)^2, & l = 1,\\ C_4\big(1 + C_0^{2l}(\Delta t)^{2l-2}\big)(\Delta t)^2, & l = 2,3,4,5, \end{cases} \tag{4.37}$$

where C_4 is independent of C_0 and Δt.

Step 3: Completion of the induction process. Recalling (3.6), we have

$$\begin{aligned} |1-\xi^{n+1}| =& \left|\frac{R(t^{k+1})}{E(\mathbf{m}(t^{n+1}))+K_0} - \frac{R^{n+1}}{E(\tilde{\mathbf{m}}^{n+1})+K_0}\right| \\ \le& C(|e_R^{n+1}| + \|\nabla \tilde{e}_{\mathbf{m}}^{n+1}\|) \\ \le& C_5\Delta t\sqrt{1 + C_0^{2q}(\Delta t)^{2q-2}}, \end{aligned} \tag{4.38}$$

where C_5 is independent of C_0 and Δt, $q = 2$ when $l = 1$, and $q = l$ when $l = 2,3,4,5$.

Letting $C_0 = \max\{\frac{(8C_1)^{4/q}}{2}, \frac{(2C_2)^{2/q}}{2}, C_3, 2C_5, 1\}$ and $\Delta t \le \frac{1}{1+2^{q+2}C_0^q}$, we can obtain

$$C_5\sqrt{1 + C_0^{2q}(\Delta t)^{2q-2}} \le C_5(1 + C_0^q\Delta t) \le C_0. \tag{4.39}$$

Then combining (4.38) with (4.39) results in

$$|1-\xi^{n+1}| \le C_0\Delta t. \tag{4.40}$$

Recalling (4.36), we have

$$\|\tilde{e}_{\mathbf{m}}^{n+1}\| + \|\nabla\tilde{e}_{\mathbf{m}}^{n+1}\| + \|\Delta\tilde{e}_{\mathbf{m}}^{n+1}\| \le \begin{cases} \sqrt{C_2\big(1 + C_0^4(\Delta t)^2\big)}(\Delta t)^{1/2}, & l = 1,\\ \sqrt{C_2\big(1 + C_0^{2l}\big)(\Delta t)^{2l-2}}(\Delta t)^{1/2}, & l = 2,3,4,5. \end{cases} \tag{4.41}$$

Thus we have

$$\|\tilde{e}_{\mathbf{m}}^{n+1}\| + \|\nabla\tilde{e}_{\mathbf{m}}^{n+1}\| + \|\Delta\tilde{e}_{\mathbf{m}}^{n+1}\| \le \sqrt{2C_2}(\Delta t)^{1/2} \le (\Delta t)^{1/4}, \tag{4.42}$$

which completes the induction process (4.4) and (4.5).

Recalling (4.36) and Lemma 5, we have the final results

$$\begin{aligned} &\|\mathbf{m}^{n+1} - \mathbf{m}(t^{n+1})\|^2 + \|\nabla(\mathbf{m}^{n+1} - \mathbf{m}(t^{n+1}))\|^2 + \|\hat{\mathbf{m}}^{n+1} - \mathbf{m}(t^{n+1})\|^2 \\ &+ \|\nabla(\hat{\mathbf{m}}^{n+1} - \mathbf{m}(t^{n+1}))\|^2 + \|\tilde{\mathbf{m}}^{n+1} - \mathbf{m}(t^{n+1})\|^2 \\ &+ \|\nabla(\tilde{\mathbf{m}}^{n+1} - \mathbf{m}(t^{n+1}))\|^2 + \Delta t\sum_{k=0}^{n}\|\Delta(\tilde{\mathbf{m}}^{k+1} - \mathbf{m}(t^{k+1}))\|^2 \le C(\Delta t)^{2l}. \end{aligned} \tag{4.43}$$

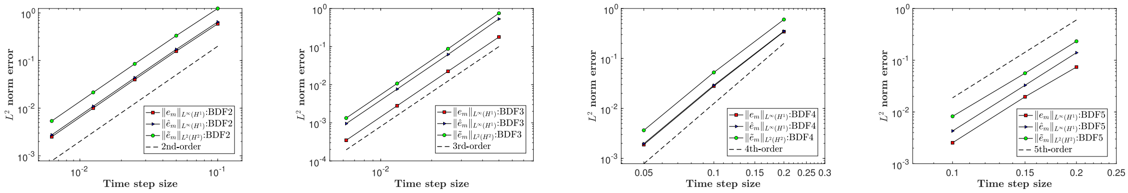

(a) BDF2 vs. errors (b) BDF3 vs. errors (c) BDF4 vs. errors (d) BDF5 vs. errors

Fig. 3. Numerical convergence rate of the second- to fifth-order schemes with $\beta = 0$ and $S = 1$ in Example 1. (For interpretation of the references to colour in this figure legend, the reader is referred to the web version of this article.)

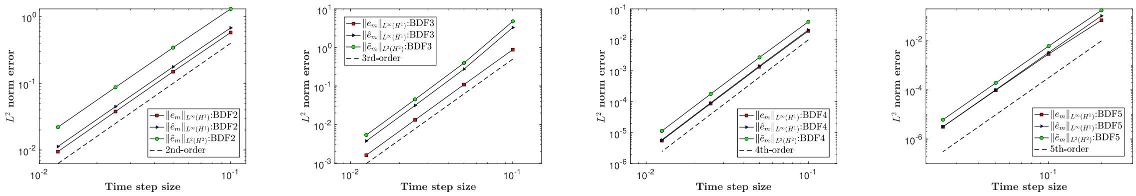

(a) BDF2 vs. errors (b) BDF3 vs. errors (c) BDF4 vs. errors (d) BDF5 vs. errors

Fig. 4. Numerical convergence rate of the second- to fifth-order schemes using the semi-implicit discretization in (5.1) with $\beta = 1$ and $S = 0$ in Example 1. (For interpretation of the references to colour in this figure legend, the reader is referred to the web version of this article.)

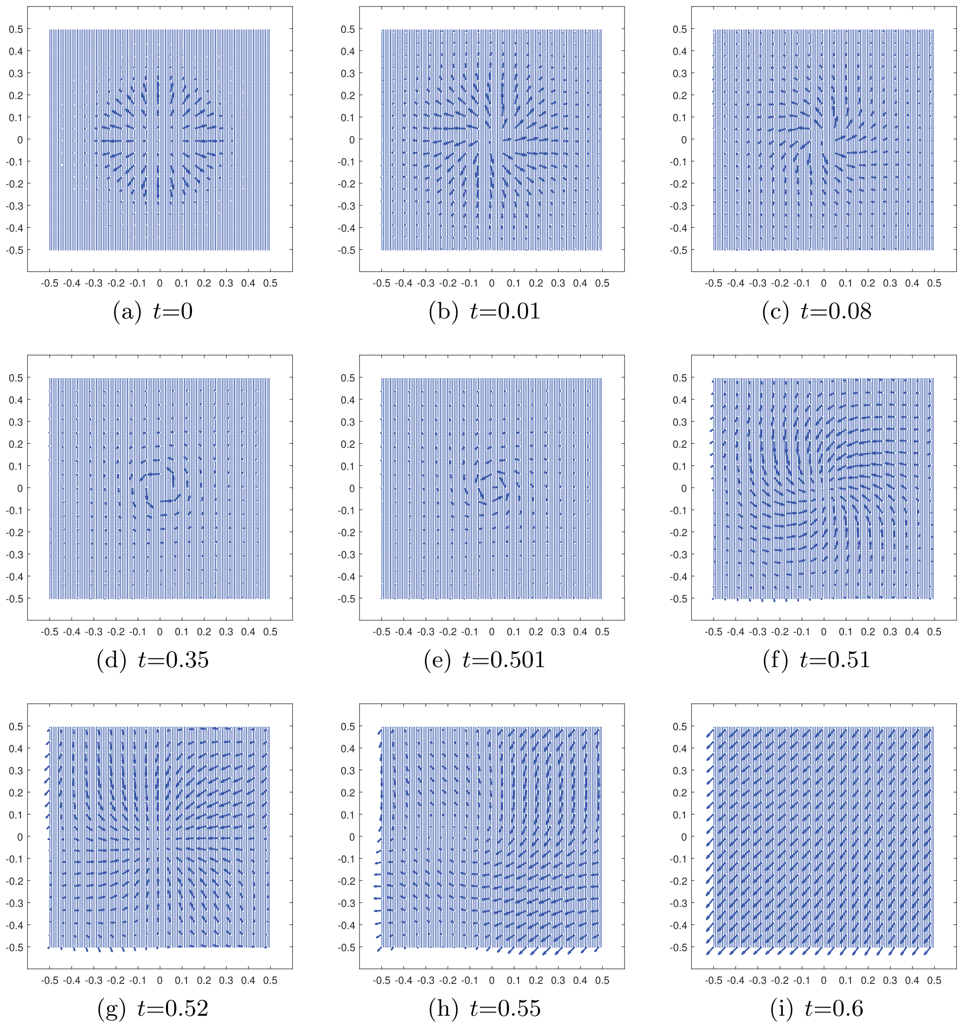

(a) t=0 (b) t=0.01 (c) t=0.08

(d) t=0.35 (e) t=0.501 (f) t=0.51

(g) t=0.52 (h) t=0.55 (i) t=0.6

Fig. 5. Numerical magnetization $\mathbf{m}$ (projected on x_1x_2-plane) with $N = 128$.

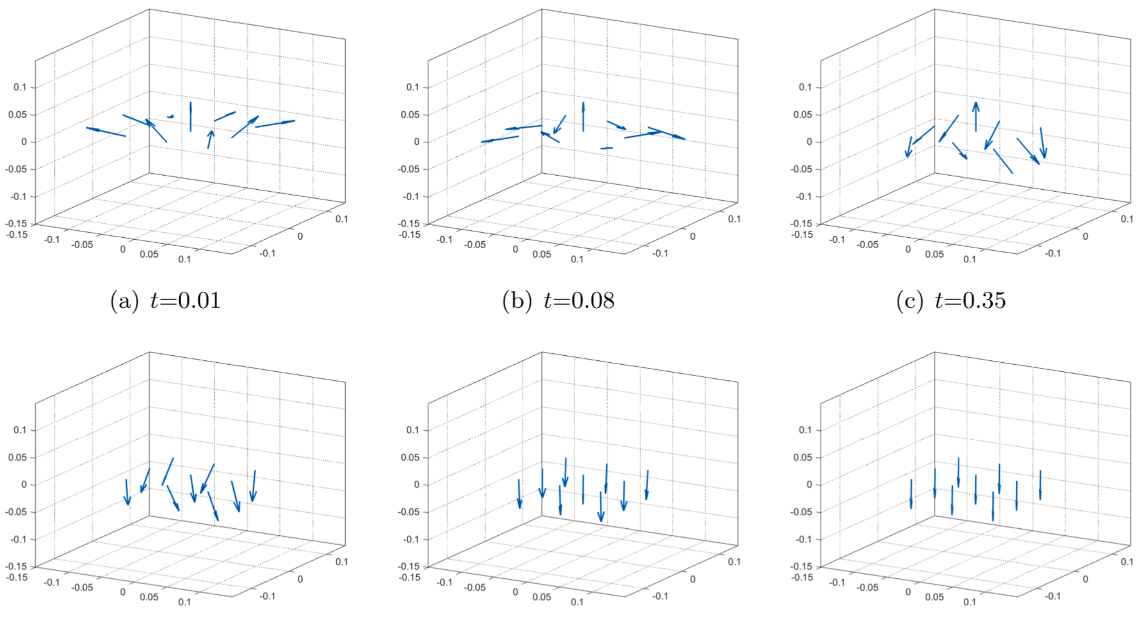

(a) t=0.01 (b) t=0.08 (c) t=0.35

(d) t=0.501 (e) t=0.51 (f) t=0.6

Fig. 6. Numerical magnetization $\mathbf{m}$ around the origin with $N = 128$.

The proof of Theorem 2 is finally completed. □

Remark 3. The high-order error estimates established in this work are based on the classical BDF-l discretizations. This framework can be readily extended to encompass general and modified BDF-l schemes, which offer improved stability properties [34–36]. In addition to multi-step IMEX numerical schemes, several IMEX Runge-Kutta schemes have been developed for the Landau-Lifshitz equation [37,38]. We would like to emphasize that the error analysis framework we have proposed for scheme (3.5)-(3.7) can be extended to the GSAV approach combined with IMEX Runge-Kutta methods by leveraging the analytical techniques established for Runge-Kutta methods, along with the higher-order consistency results discussed in [37,38].

5. Semi-implicit discretization for the term $\beta \mathbf{m} \times \Delta \mathbf{m}$

In the last section, we established error estimates for the scheme (3.5) where the term $\beta \mathbf{m} \times \Delta \mathbf{m}$ is treated explicitly under the condition (4.3). In order to relax this condition, we shall treat the term $\beta \mathbf{m} \times \Delta \mathbf{m}$ semi-implicitly, namely. In this case we do not need to add the stabilization term. So we replace (3.5) by

$$D_l \tilde{\mathbf{m}}^{n+1} = \gamma \Delta \tilde{\mathbf{m}}^{n+1} + \gamma |\nabla B_l(\mathbf{m}^n)|^2 B_l(\mathbf{m}^n) - \beta B_l(\mathbf{m}^n) \times \Delta \tilde{\mathbf{m}}^{n+1}. \tag{5.1}$$

We establish below an error analysis for the above scheme under a condition which is less restrictive than (4.3), at the price of having to solve the elliptic system with variable coefficients at each time step.

The main result of this section is stated below.

Theorem 3. *Supposing that the damping parameter γ satisfies*

$$\gamma > \frac{|\beta| \tau_l}{1 - \tau_l} \tag{5.2}$$

and assuming $\boldsymbol{m} \in H^{l+1}(0,T; \boldsymbol{L}^2(\Omega)) \bigcap H^l(0,T; \boldsymbol{W}^{1,3}(\Omega)) \bigcap L^\infty(0,T; H^4(\Omega))$, then for the scheme (5.1), (3.6)-(3.8), we have

$$\begin{aligned}
&\|\boldsymbol{m}^{n+1} - \boldsymbol{m}(t^{n+1})\|^2 + \|\nabla(\boldsymbol{m}^{n+1} - \boldsymbol{m}(t^{n+1}))\|^2 + \|\hat{\boldsymbol{m}}^{n+1} - \boldsymbol{m}(t^{n+1})\|^2 \\
&+ \|\nabla(\hat{\boldsymbol{m}}^{n+1} - \boldsymbol{m}(t^{n+1}))\|^2 + \|\tilde{\boldsymbol{m}}^{n+1} - \boldsymbol{m}(t^{n+1})\|^2 \\
&+ \|\nabla(\tilde{\boldsymbol{m}}^{n+1} - \boldsymbol{m}(t^{n+1}))\|^2 + \Delta t \sum_{k=0}^{n} \|\Delta(\tilde{\boldsymbol{m}}^{k+1} - \boldsymbol{m}(t^{k+1}))\|^2 \\
\leq & C(\Delta t)^{2l}, \quad \forall\, 0 \leq n \leq N-1, \quad 1 \leq l \leq 5,
\end{aligned} \tag{5.3}$$

where C is a positive constant independent of Δt.

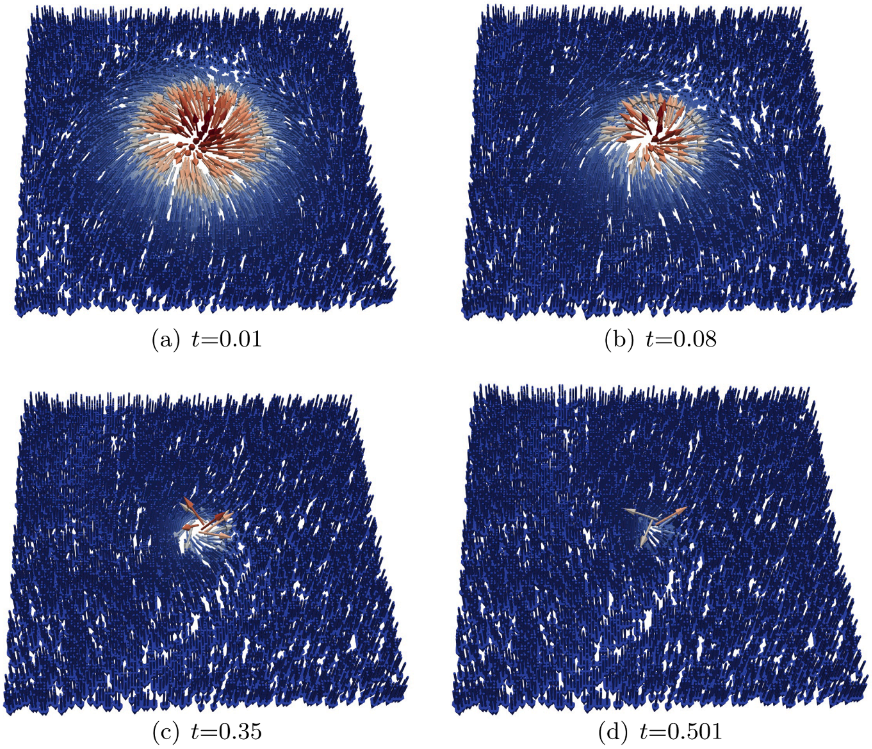

Fig. 7. Three-dimensional magnetization visualization with $N = 128$.

Proof. The proof of Theorem 3 is exactly the same as Theorem 2, except for the highly nonlinear term with exchange parameter $\beta \neq 0$, so for the sake of brevity our focus will be on this. Similar to (4.26), we can obtain

$$\begin{aligned}|I_6| =&|\beta|\left|\left((\mathbf{m}(t^{k+1}) - B_l(\mathbf{m}(t^k))) \times \Delta\tilde{e}_{\mathbf{m}}^{k+1}, \Delta\tilde{e}_{\mathbf{m}}^{k+1} - \tau_l \Delta\tilde{e}_{\mathbf{m}}^{k}\right)\right| \\ &+ |\beta|\left|\left((\mathbf{m}(t^{k+1}) - B_l(\mathbf{m}(t^k))) \times \Delta\mathbf{m}(t^{k+1}), \Delta\tilde{e}_{\mathbf{m}}^{k+1} - \tau_l \Delta\tilde{e}_{\mathbf{m}}^{k}\right)\right| \\ &+ |\beta|\left|\left(B_l(e_{\mathbf{m}}^{k}) \times \Delta\tilde{e}_{\mathbf{m}}^{k+1}, \Delta\tilde{e}_{\mathbf{m}}^{k+1} - \tau_l \Delta\tilde{e}_{\mathbf{m}}^{k}\right)\right| + |\beta|\left|\left(B_l(e_{\mathbf{m}}^{k}) \times \Delta\mathbf{m}(t^{k+1}), \Delta\tilde{e}_{\mathbf{m}}^{k+1} - \tau_l \Delta\tilde{e}_{\mathbf{m}}^{k}\right)\right| \\ &+ |\beta|\left|\left(\mathbf{m}(t^{k+1}) \times \Delta\tilde{e}_{\mathbf{m}}^{k+1}, \Delta\tilde{e}_{\mathbf{m}}^{k+1} - \tau_l \Delta\tilde{e}_{\mathbf{m}}^{k}\right)\right|.\end{aligned} \tag{5.4}$$

Applying Cauchy-Schwarz inequality, the first term on the right hand side of (5.4) can be estimated by

$$\begin{aligned}&\beta\left|\left((\mathbf{m}(t^{k+1}) - B_l(\mathbf{m}(t^k))) \times \Delta\tilde{e}_{\mathbf{m}}^{k+1}, \Delta\tilde{e}_{\mathbf{m}}^{k+1} - \tau_l \Delta\tilde{e}_{\mathbf{m}}^{k}\right)\right| \\ \le&|\beta|\| \sum_{i=1}^{l} d_i \int_{k+1-i}^{k+1} (t^{k+1-i} - s)^{l-1} \frac{\partial^l \mathbf{m}}{\partial t^l}(s) ds\|_{L^\infty} \|\Delta\tilde{e}_{\mathbf{m}}^{k+1}\|_{L^2} \|\tau_l \Delta\tilde{e}_{\mathbf{m}}^{k}\|_{L^2} \\ \le&\epsilon\|\Delta\tilde{e}_{\mathbf{m}}^{k}\|_{L^2}^2 + C(\Delta t)^{2l-1} \int_{k+1-l}^{k+1} \|\frac{\partial^l \mathbf{m}}{\partial t^l}(s)\|_{H^2}^2 ds \|\Delta\tilde{e}_{\mathbf{m}}^{k+1}\|_{L^2}^2 \\ \le&\epsilon\|\Delta\tilde{e}_{\mathbf{m}}^{k}\|_{L^2}^2 + \epsilon\|\Delta\tilde{e}_{\mathbf{m}}^{k+1}\|_{L^2}^2,\end{aligned} \tag{5.5}$$

where we set $\Delta t \le \hat{C}$, which is sufficiently small to keep the last inequality holds.

Applying the interpolation inequality (2.6), the second term on the right hand side of (5.4) can be bounded by

$$\begin{aligned}&\beta\left|\left((\mathbf{m}(t^{k+1}) - B_l(\mathbf{m}(t^k))) \times \Delta\mathbf{m}(t^{k+1}), \Delta\tilde{e}_{\mathbf{m}}^{k+1} - \tau_l \Delta\tilde{e}_{\mathbf{m}}^{k}\right)\right| \\ \le&|\beta|\| \sum_{i=1}^{l} d_i \int_{k+1-i}^{k+1} (t^{k+1-i} - s)^{l-1} \frac{\partial^l \mathbf{m}}{\partial t^l}(s) ds\|_{L^\infty} \|\Delta\mathbf{m}(t^{k+1})\|_{L^2} \|\Delta\tilde{e}_{\mathbf{m}}^{k+1} - \tau_l \Delta\tilde{e}_{\mathbf{m}}^{k}\|_{L^2} \\ \le&\epsilon\|\Delta\tilde{e}_{\mathbf{m}}^{k+1}\|_{L^2}^2 + \epsilon\|\Delta\tilde{e}_{\mathbf{m}}^{k}\|_{L^2}^2 + C(\Delta t)^{2l-1} \int_{k+1-l}^{k+1} \|\frac{\partial^l \mathbf{m}}{\partial t^l}(s)\|_{H^2}^2 ds.\end{aligned} \tag{5.6}$$

Using the interpolation inequality (2.6) and (4.7), the third and fourth terms on the right hand side of (5.4) can be transformed into

$$\begin{aligned}
&\beta\Big|\big(B_l(e_{\mathbf{m}}^k)\times\Delta\tilde{e}_{\mathbf{m}}^{k+1},\Delta\tilde{e}_{\mathbf{m}}^{k+1}-\tau_l\Delta\tilde{e}_{\mathbf{m}}^k\big)\Big|+\beta\Big|\big(B_l(e_{\mathbf{m}}^k)\times\Delta\mathbf{m}(t^{k+1}),\Delta\tilde{e}_{\mathbf{m}}^{k+1}-\tau_l\Delta\tilde{e}_{\mathbf{m}}^k\big)\Big|\\
\le&\beta\|B_l(e_{\mathbf{m}}^k)\|_{L^\infty}\|\Delta\tilde{e}_{\mathbf{m}}^{k+1}\|_{L^2}\|\tau_l\Delta\tilde{e}_{\mathbf{m}}^k\|_{L^2}+\beta\|B_l(e_{\mathbf{m}}^k)\|_{L^\infty}\|\Delta\mathbf{m}(t^{k+1})\|_{L^2}\|\Delta\tilde{e}_{\mathbf{m}}^{k+1}-\tau_l\Delta\tilde{e}_{\mathbf{m}}^k\|_{L^2}\\
\le&\beta\|B_l(e_{\mathbf{m}}^k)\|_{H^1}^{1/2}\|B_l(e_{\mathbf{m}}^k)\|_{H^2}^{1/2}(\|\Delta\tilde{e}_{\mathbf{m}}^{k+1}\|_{L^2}\|\tau_l\Delta\tilde{e}_{\mathbf{m}}^k\|_{L^2}+\|\Delta\mathbf{m}(t^{k+1})\|_{L^2}\|\Delta\tilde{e}_{\mathbf{m}}^{k+1}-\tau_l\Delta\tilde{e}_{\mathbf{m}}^k\|_{L^2})\\
\le&\epsilon\|\Delta\tilde{e}_{\mathbf{m}}^{k+1}\|_{L^2}^2+\frac{\epsilon}{l}\sum_{i=0}^{l-1}\|\Delta\tilde{e}_{\mathbf{m}}^{k-i}\|_{L^2}^2+C(\Delta t)^{1/4}\|\Delta\tilde{e}_{\mathbf{m}}^k\|_{L^2}^2+C\|\nabla B_l(\tilde{e}_{\mathbf{m}}^k)\|_{L^2}^2\\
\le&\epsilon\|\Delta\tilde{e}_{\mathbf{m}}^{k+1}\|_{L^2}^2+\frac{\epsilon}{l}\sum_{i=0}^{l-1}\|\Delta\tilde{e}_{\mathbf{m}}^{k-i}\|_{L^2}^2+\epsilon\|\Delta\tilde{e}_{\mathbf{m}}^k\|_{L^2}^2+C\|\nabla B_l(\tilde{e}_{\mathbf{m}}^k)\|_{L^2}^2,
\end{aligned}\tag{5.7}$$

where we set $\Delta t\le\check{C}$, which is sufficiently small to keep the last inequality holds.

Recalling the fact that $\|\mathbf{m}(t^{k+1})\|_{L^\infty}=1$, the last term on the right hand side of (5.4) can be estimated by

$$\begin{aligned}
&\beta\Big|\big(\mathbf{m}(t^{k+1})\times\Delta\tilde{e}_{\mathbf{m}}^{k+1},\Delta\tilde{e}_{\mathbf{m}}^{k+1}-\tau_l\Delta\tilde{e}_{\mathbf{m}}^k\big)\Big|=\beta\Big|\big(\mathbf{m}(t^{k+1})\times\Delta\tilde{e}_{\mathbf{m}}^{k+1},-\tau_l\Delta\tilde{e}_{\mathbf{m}}^k\big)\Big|\\
\le&|\beta|\tau_l\|\mathbf{m}(t^{k+1})\|_{L^\infty}\|\Delta\tilde{e}_{\mathbf{m}}^{k+1}\|_{L^2}\|\Delta\tilde{e}_{\mathbf{m}}^k\|_{L^2}\\
\le&\frac{|\beta|\tau_l}{2}\|\Delta\tilde{e}_{\mathbf{m}}^{k+1}\|_{L^2}^2+\frac{|\beta|\tau_l}{2}\|\Delta\tilde{e}_{\mathbf{m}}^k\|_{L^2}^2.
\end{aligned}\tag{5.8}$$

Thus by using the similar procedure for the fully explicit case in (4.33), we can obtain that

$$\begin{aligned}
&\sum_{i,j=1}^{l}g_{i,j}(\nabla\tilde{e}_{\mathbf{m}}^{k+1+i-l},\nabla\tilde{e}_{\mathbf{m}}^{k+1+j-l})-\sum_{i,j=1}^{l}g_{i,j}(\nabla\tilde{e}_{\mathbf{m}}^{k+i-l},\nabla\tilde{e}_{\mathbf{m}}^{k+j-l})\\
&+\|\sum_{i=0}^{l}\theta_i\nabla\tilde{e}_{\mathbf{m}}^{k+1+i-l}\|^2+\frac{\gamma(2-\tau_l)-|\beta|\tau_l}{2}\Delta t\|\Delta\tilde{e}_{\mathbf{m}}^{k+1}\|^2
\end{aligned}\tag{5.9}$$

$$\begin{aligned}
\le&7\epsilon\Delta t\|\Delta\tilde{e}_{\mathbf{m}}^{k+1}\|_{L^2}^2+(6\epsilon+\frac{\gamma\tau_l+|\beta|\tau_l}{2})\Delta t\|\Delta\tilde{e}_{\mathbf{m}}^k\|_{L^2}^2+\frac{2\epsilon}{l}\sum_{i=0}^{l-1}\Delta t\|\Delta\tilde{e}_{\mathbf{m}}^{k-i}\|_{L^2}^2\\
&+C\Delta t\|\nabla B_l(\tilde{e}_{\mathbf{m}}^k)\|_{L^2}^2+C\Delta t(C_0\Delta t)^{2q}+C\Delta t\|\nabla B_l(\mathbf{m}(t^k))\|_{L^6}^4\|\nabla B_l(\tilde{e}_{\mathbf{m}}^k)\|_{L^2}^2\\
&+C(\Delta t)^{2l}\int_{k+1-l}^{k+1}\left(\|\frac{\partial^l\mathbf{m}}{\partial t^l}(s)\|_{W^{1,3}}^2+\|\frac{\partial^{l+1}\mathbf{m}}{\partial t^{l+1}}(s)\|_{L^2}^2+\|\frac{\partial^l\mathbf{m}}{\partial t^l}(s)\|_{H^2}^2\right)ds,
\end{aligned}\tag{5.10}$$

Using the condition (5.2) and setting $\epsilon=\frac{\gamma(1-\tau_l)-|\beta|\tau_l}{30}$, we have

$$\gamma(1-\tau_l)-|\beta|\tau_l-15\epsilon>0.$$

Summing (5.9) over k from 0 to n and applying the discrete Gronwall Lemma 3, we can arrive at

$$\|\nabla\tilde{e}_{\mathbf{m}}^{n+1}\|^2+\Delta t\sum_{k=0}^{n}\|\Delta\tilde{e}_{\mathbf{m}}^{k+1}\|^2\le\begin{cases}C_1\big(1+C_0^4(\Delta t)^2\big)(\Delta t)^2, & l=1,\\ C_1\big(1+C_0^{2l}\big)(\Delta t)^{2l}, & l=2,3,4,5,\end{cases}\tag{5.11}$$

where C_1 is independent of C_0 and Δt. Then using exactly the similar procedure in Steps 2 and 3 in Section 4, we can easily obtain the desired result (5.3). □

6. Numerical experiments

In this section, we carry out some numerical experiments to verify the accuracy and stability of the high-order IMEX-GSAV schemes (3.5)-(3.8) for the Landau-Lifshitz equation. We assume periodic boundary conditions and use the Fourier-spectral method for spatial discretization, which reduces the equation (3.5) to a diagonal system in the frequency space so it can be easily implemented.

6.1. Convergence rate with a known exact solution

We test the convergence rate for the Landau-Lifshitz Eq. (2.3) with an external force so that the exact solution is

$$\begin{aligned}
m_1^e(x,y,t)=&\sin(t+x)\cos(t+y),\\
m_2^e(x,y,t)=&\cos(t+x)\cos(t+y),\\
m_3^e(x,y,t)=&\sin(t+y).
\end{aligned}\tag{6.1}$$

We set $\gamma=1$, $K_0=1$ and $\Omega=[0,2\pi)^2$ with periodic boundary conditions and use the Fourier-spectral method with 64×64 modes for spatial approximation so that the spatial discretization error is negligible. For the case of $\beta=0$ and $S=0$, we plot in Figs. 1(a)-1(d) the convergence rates in $l^\infty(0,T;H^1(\Omega))\bigcap l^2(0,T;H^2(\Omega))$ with $l=2,\ 3,\ 4,\ 5$ at $T=2$, which are in good agreement with Theorem 2. We also conducted a numerical experiment to investigate whether replacing the BDF-l temporal stencil $\tilde{\mathbf{m}}^{n-k}$, $(k=1,2,\dots,l-1)$ in

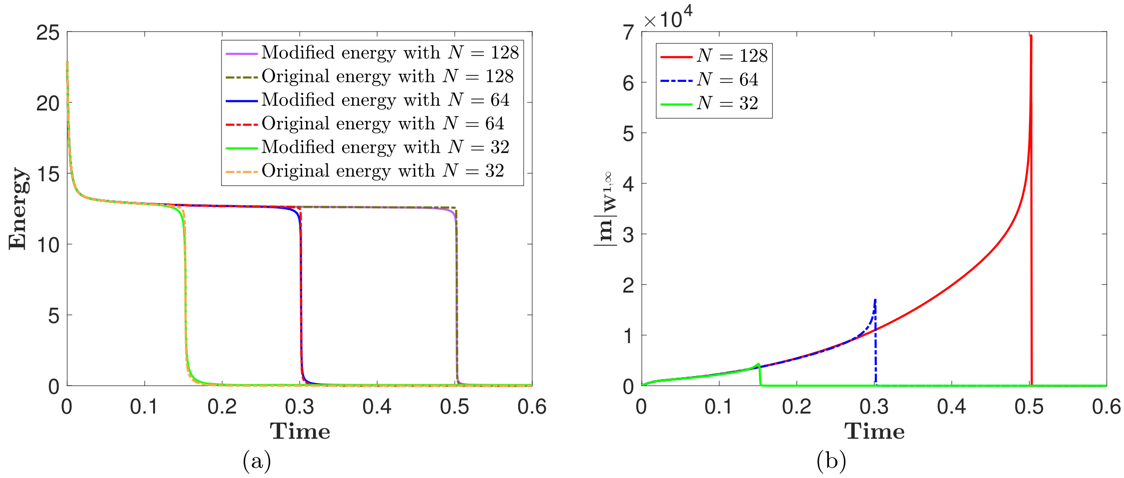

Fig. 8. Evolutions of energy (left) and $|\mathbf{m}|_{W^{1,\infty}}$ (right) computed with different Fourier modes.

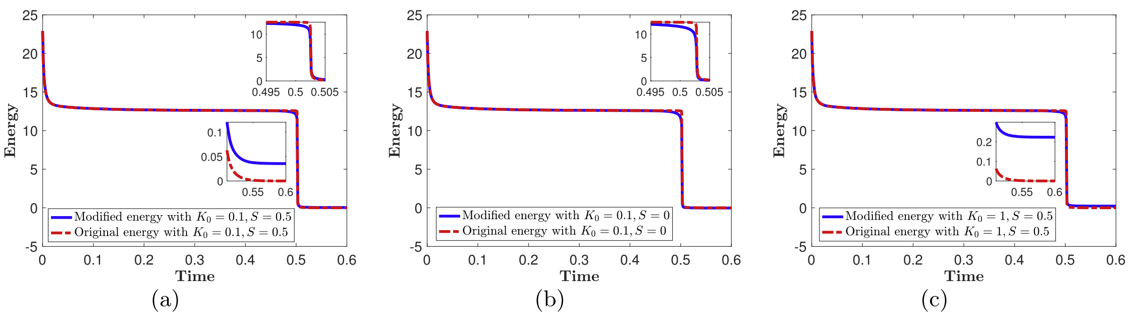

Fig. 9. Evolutions of energy computed with different parameters K_0 and S . (For interpretation of the references to colour in this figure legend, the reader is referred to the web version of this article.)

(3.9)-(3.11) with the original magnetization vector variables from previous time steps $\mathbf{m}^{n-k}$, $(k = 1, 2, \dots, l-1)$ would yield essentially different computational results for the proposed schemes. The results of this alternative approach are presented in Fig. 2(a)-2(d). A comparison with Fig. 1 indicates that using the original magnetization variables results in slightly smaller numerical errors. However, this substitution introduces considerable challenges for the theoretical analysis of high-order schemes in time. Therefore, we adhere to the formulation specified in (3.9)-(3.11) for the remainder of this paper. We also test the convergence rates for $\beta = 0$ and $S = 1$, with results shown in Figs. 3(a)-3(d). By comparing these to the $S = 0$ case (Figs. 1(a)-1(d)), we observe that the addition of the stabilization term introduces additional error. Additionally, Figs. 4(a)-4(d) plot the convergence rates for the second- to fifth-order schemes, which use the semi-implicit discretization in (5.1) for the $\beta = 1$ and $S = 0$ case. The results show that the semi-implicit discretization performs well for the $\beta = 1$ case.

6.2. *Phenomenon of blow up*

As indicated in [11,18,39], when the initial value is sufficiently smooth, it is known that (1.1) has a unique smooth solution in short time which may blow up at some finite time. So we investigate the possible blowup of the general Landau-Lifshitz Eq. (1.1) with certain smooth initial condition in this subsection. The initial data $\mathbf{m}_0$ is defined by

$$\mathbf{m}_0(\mathbf{x}) = \begin{cases} (0, 0, -1)^{\mathrm{T}}, & |\mathbf{x}| > \dfrac{1}{2}, \\ \left(\dfrac{2x_1 A}{A^2 + |\mathbf{x}|^2}, \dfrac{2x_2 A}{A^2 + |\mathbf{x}|^2}, \dfrac{A^2 - |\mathbf{x}|^2}{A^2 + |\mathbf{x}|^2}\right)^{\mathrm{T}}, & |\mathbf{x}| \le \dfrac{1}{2}, \end{cases} \tag{6.2}$$

where $A = (1 - 2|\mathbf{x}|)^4$. For spatial approximation in the domain $\Omega = [-1/2, 1/2)^2$, we use Fourier modes in each direction. The parameters are set as $\Delta t = 10^{-6}$, $\gamma = 1$, $S = 0.5$, $\beta = 1$ and $K_0 = 0.1$.

Numerical simulation for the orthogonal projection of the vector field $\mathbf{m}^{n+1}$ on the x_1x_2−plane and close-up pictures of $\mathbf{m}^{n+1}$ near the origin at $t = 0$, 0.01, 0.08, 0.35, 0.501, 0.51, 0.52, 0.55, 0.6 are shown in Figs. 5- 7 by using (3.5)-(3.8) with $l = 2$. It can be observed that $\mathbf{m}^{n+1}$ preserves $(0, 0, 1)^{\mathrm{T}}$ at the origin and gradually turns down to $(0, 0, -1)^{\mathrm{T}}$ near the origin, which is consistent with the phenomenon of blowup presented in [11,18]. We can observe that the energy dissipation law is preserved well in Fig. 6.2(a) with

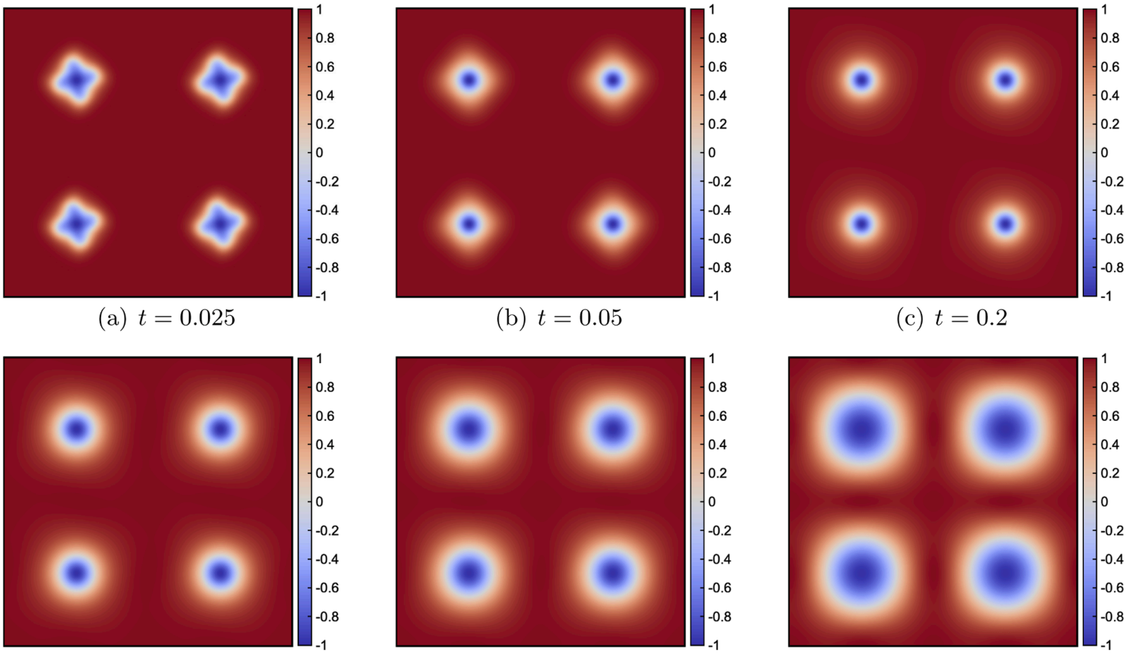

(a) $t = 0.025$ (b) $t = 0.05$ (c) $t = 0.2$

(d) $t = 0.4$ (e) $t = 0.5$ (f) $t = 4$

Fig. 10. Time evolution of out-of-plane magnetization component (m_3) showing skyrmion lattice formation. Initial nucleation domains evolve into stable skyrmion cores at $t = 4$.

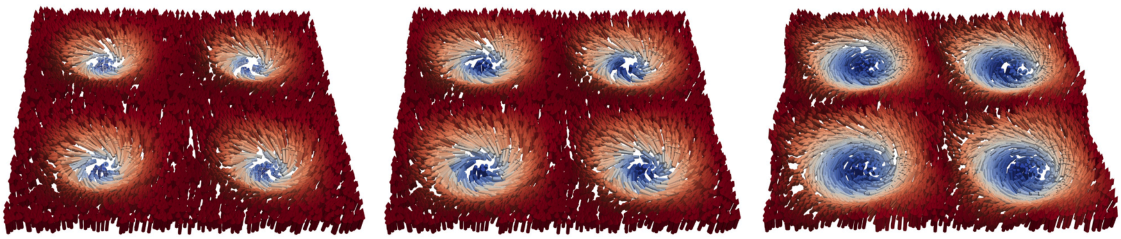

(a) $t = 0.4$ (b) $t = 0.5$ (c) $t = 4$

Fig. 11. Three-dimensional magnetization visualization during lattice formation .

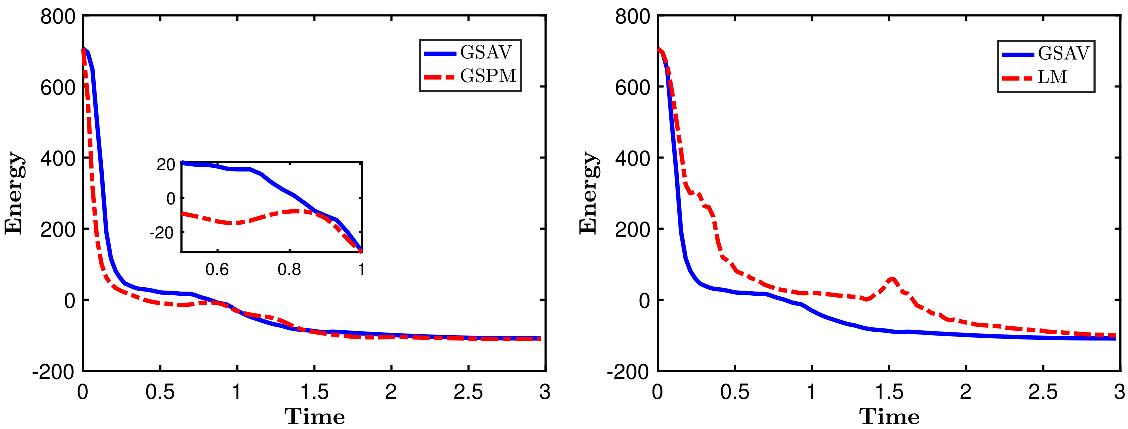

(a) Comparison with the GSPM scheme [42]. (b) Comparison with the LM scheme [15].

Fig. 12. Comparison of the discrete energy evolution between the proposed IMEX-GSAV scheme and existing schemes with a large time step $\Delta t = 3 \times 10^{-2}$. (For interpretation of the references to colour in this figure legend, the reader is referred to the web version of this article.)

different Fourier modes $N = 32, 64, 128$. In Fig. 6, we plot the evolution of $|\mathbf{m}|_{W^{1,\infty}}$ with respect to time, which indicate that the gradient of $\mathbf{m}^{n+1}$ near the origin appears to going to infinity as we refine the mesh. Thus the solution of the Landau-Lifshitz Eq. (1.1) with this smooth initial data may blow up around the origin in a finite time.

We also investigate the influence of the stabilization parameter K_0 on the numerical performance. The selection of K_0 is constrained by the requirement that the scalar auxiliary variable R, defined in (3.1), must remain positive throughout the simulation. As illustrated in Figs. 9(a) and 9(c), a comparison of different K_0 values reveals that a smaller K_0 leads to a closer approximation between the modified energy and the original physical energy. Consequently, in practical computations, we recommend selecting a small K_0 value to minimize the deviation of the modified energy, as long as the positivity of R is strictly preserved. We now investigate the stabilization parameter S. In Figs. 9(a) and 9(b), we compare the evolution of the original energy E and the modified energy R using $S = 0.5$ and $S = 0$, respectively. A key observation occurs around $t = 0.5$, where the system experiences a rapid change in energy. In the case without stabilization ($S = 0$, Fig. 9(b)), a noticeable deviation between R and E appears during this transition. Conversely, when stabilization is active ($S = 0.5$, Fig. 9(a)), the modified energy R provides a significantly closer approximation to the original energy E. This result demonstrates that, in addition to guaranteeing long-term numerical stability, the stabilization term S can also enhance the accuracy of the modified energy, particularly when the system dynamics are changing rapidly.

6.3. Skyrmion lattice dynamics in micromagnetic modeling

The temporal evolution of magnetization in micromagnetics is governed by the Landau-Lifshitz equation. This section presents numerical investigations of magnetic skyrmion lattice formation through extended micromagnetic modeling. Motivated by the particle-like behavior of skyrmions that induces collective ordering through inter-skyrmion interactions, we implement the dimensionless Landau-Lifshitz [40,41] dynamics under periodic boundary conditions:

$$\frac{\partial \mathbf{m}}{\partial t} = -\beta \mathbf{m} \times \mathbf{h}_{\text{eff}} - \gamma \mathbf{m} \times \left(\mathbf{m} \times \mathbf{h}_{\text{eff}}\right), \tag{6.3}$$

where the dimensionless damping parameter $\gamma > 0$ controls relaxation dynamics. We introduce the energy functional.

$$E(\mathbf{m}) = \int_\Omega \left(\frac{1}{2}|\nabla \mathbf{m}|^2 + \mathcal{D}(\nabla \times \mathbf{m}) \cdot \mathbf{m} + \Phi(\mathbf{m}) - \mu_0 \mathbf{H}_{\text{ex}} \cdot \mathbf{m}\right) d\mathbf{x}.$$

Here, $\mathcal{D}$ represents the Dzyaloshinskii-Moriya interaction (DMI) strength, while $\Phi(\mathbf{m})$ is the anisotropy energy, and for simplicity the material is assumed to be uniaxial with $\Phi(\mathbf{m}) = K_u(m_2^2 + m_3^2)$. The final term represents the Zeeman energy arising from the external magnetic field $\mathbf{H}_{\text{ex}} = (0, 0, 1)$, with μ_0 denoting the permeability of vacuum. It is straightforward to derive the following energy stability

$$\frac{\mathrm{d}E(\mathbf{m}(t))}{\mathrm{d}t} = -\gamma \left\|\mathbf{m} \times \mathbf{h}_{\text{eff}}\right\|^2.$$

Correspondingly, the effective field is derived from the gradient of the energy functional

$$\mathbf{h}_{\text{eff}} = -\frac{\delta E}{\delta \boldsymbol{m}} = \Delta \boldsymbol{m} - 2\mathcal{D}\nabla \times \boldsymbol{m} + 2K_u\left(\boldsymbol{e}_3 \otimes \boldsymbol{e}_3\right)\boldsymbol{m} + \mu_0 \mathbf{H}_{\text{ex}}.$$

Our lattice formation protocol initializes four $\pi/4$-sized square domains centered at quadrant midpoints in $\Omega = (0, 2\pi]^2$, with out-of-plane magnetization $[0, 0, -1]$ contrasting the $[0, 0, 1]$ background. The dimensionless parameters $\beta = 1$, $\gamma = 0.6$, $\mathcal{D} = 1$, $K_u = -0.2$, $\mu_0 = 0.2$ were selected to stabilize skyrmions. Numerical simulations employ a -spectral method with 256×256 modes, using a time step of $\Delta t = 5 \times 10^{-3}$. Fig. 10 demonstrates the emergence of four stable skyrmions at $t = 4$, confirming lattice stabilization. The transient dynamics revealed in Fig. 11 through 3D magnetization snapshots at $t = 0.4, 0.5, 4$ illustrate the evolution from initial domain configuration to ordered lattice. Notably, the m_3-component evolution in Fig. 10 exhibits characteristic skyrmion core formation and stabilization processes.

6.3.1. Comparisons with existing schemes

Since many existing works for this equation rely on semi-implicit schemes, our proposed IMEX-GSAV scheme, which occasionally incorporates the Gauss-Seidel method for certain complex energy formulations as described in Remark 1, offers a substantial improvement in computational efficiency as it is solved fully explicitly. Therefore, we compare our method with two explicit schemes, such as the Gauss-Seidel projection method (GSPM) [31] and the length preserving scheme using the Lagrange multiplier approach (LM) [7]. We test the robustness of these schemes using a relatively large time step $\Delta t = 3 \times 10^{-2}$. The other parameters are set as $\beta = 1$, $\gamma = 0.1$, $\mathcal{D} = 2$, $K_u = -2$, $\mu_0 = 0.2$, and $S = 1$.

- Comparison with GSPM [31]: From Fig. 12(a), we observe that the energy of the GSPM increases during the interval $[0.6, 1]$. In contrast, under the same time step $\Delta t = 3 \times 10^{-2}$, our IMEX-GSAV method still maintains energy dissipation.
- Comparison with LM [7]: We note that while LM energy-dissipative scheme can theoretically guarantee energy dissipation, it requires solving a nonlinear algebraic equation, which may require a small time step to guarantee the existence of the solution [42]. Therefore, we compare our method with the Lagrange multiplier (LM) length-preserving numerical scheme from [7]. From Fig. 6, we find that the energy of the LM scheme increases during the interval $[1.4, 1.6]$. Under the same time step $\Delta t = 3 \times 10^{-2}$, our IMEX-GSAV method still maintains energy dissipation.

These results confirm that among efficient, linear and decoupled schemes, the proposed IMEX-GSAV method offers robustness and stability allowing for larger time steps.

7. Concluding remarks

We constructed a new class of high-order implicit-explicit (IMEX) schemes based on the GSAV approach for the Landau-Lifshitz equation. These schemes are linear, length preserving, and at each time step only require solving (a) elliptic equations with constant coefficients when the nonlinear term is treated fully explicitly, or (b) elliptic system with variable coefficients when the nonlinear term is treated semi-implicitly. Furthermore, their modified energies are unconditionally decreasing, and their numerical solutions are unconditionally bounded in $l^\infty(0,T;H^1(\Omega))$. We also established rigorous error estimates up to fifth-order for these schemes in $l^\infty(0,T;H^1(\Omega))\bigcap l^2(0,T;H^2(\Omega))$. We also presented ample numerical examples, including some challenging benchmark problems, to validate the accuracy and robustness of the proposed schemes.

To the best of our knowledge, these are the first higher than second-order error estimates for schemes which enforce normalization of the magnetization. Although we only considered semi-discrete (in time) case in this paper, these schemes can be easily implemented with finite difference or spectral methods, and it is expected that the analysis can be extended, albeit tedious, to fully discrete schemes with Galerkin type spatial discretizations.

CRediT authorship contribution statement

Xiaoli Li: Writing – original draft, Methodology, Formal analysis, Conceptualization; **Jie Shen:** Writing – review & editing, Methodology, Funding acquisition, Formal analysis, Conceptualization; **Nan Zheng:** Writing – review & editing, Validation, Methodology, Investigation, Formal analysis.

Data availability

No data was used for the research described in the article.

Declaration of competing interest

The authors declare that they have no known competing financial interests or personal relationships that could have appeared to influence the work reported in this paper.

Appendix A. Error estimates for the auxiliary variable ξ^{n+1}

In this section, we give error estimates for the auxiliary variable ξ^{n+1} in (3.6).

Lemma 6. *Assuming $\boldsymbol{m}\in H^{l+1}(0,T;\boldsymbol{L}^2(\Omega))\bigcap H^l(0,T;\boldsymbol{W}^{1,3}(\Omega))\bigcap L^\infty(0,T;H^4(\Omega))$, then for the scheme (3.5)-(3.8), we have*

$$|e_R^{n+1}|^2\le\begin{cases}C_4\big(1+C_0^4(\Delta t)^2\big)(\Delta t)^2, & l=1,\\ C_4\big(1+C_0^{2l}(\Delta t)^{2l-2}\big)(\Delta t)^2, & l=2,3,4,5,\end{cases}\tag{A.1}$$

where C_4 is independent of C_0 and Δt.

Proof. Let $\mathbf{S}_R^{k+1}$ be the truncation error defined by

$$\mathbf{S}_R^{k+1}=\frac{\partial R(t^{k+1})}{\partial t}-\frac{R(t^{k+1})-R(t^k)}{\Delta t}=\frac{1}{\Delta t}\int_{t^k}^{t^{k+1}}(t^k-t)\frac{\partial^2 R}{\partial t^2}dt.\tag{A.2}$$

Subtracting (3.6) from (3.3) at t^{k+1}, we obtain the error equation corresponding to (3.6):

$$\begin{aligned}\frac{e_R^{k+1}-e_R^k}{\Delta t}&=-\frac{R(t^{k+1})}{E(\mathbf{m}(t^{k+1}))+K_0}\|\mathbf{m}(t^{k+1})\times\Delta\mathbf{m}(t^{k+1})\|^2\\&\quad+\frac{R^{k+1}}{E(\tilde{\mathbf{m}}^{k+1})+K_0}\|B_l(\mathbf{m}^k)\times\Delta\tilde{\mathbf{m}}^{k+1}\|^2-\mathbf{S}_R^{k+1}\\&=-\xi^{n+1}\big(\|\mathbf{m}(t^{k+1})\times\Delta\mathbf{m}(t^{k+1})\|^2-\|B_l(\mathbf{m}^k)\times\Delta\tilde{\mathbf{m}}^{k+1}\|^2\big)\\&\quad-R(t^{k+1})\left(\frac{1}{E(\mathbf{m}(t^{k+1}))+K_0}-\frac{1}{E(\tilde{\mathbf{m}}^{k+1})+K_0}\right)\|\mathbf{m}(t^{k+1})\times\Delta\mathbf{m}(t^{k+1})\|^2-\mathbf{S}_R^{k+1}\\&\quad-\frac{e_R^{k+1}}{E(\tilde{\mathbf{m}}^{k+1})+K_0}\|\mathbf{m}(t^{k+1})\times\Delta\mathbf{m}(t^{k+1})\|^2.\end{aligned}\tag{A.3}$$

Using (3.13) and the Sobolev embedding inequality (3.28) in [43], the first term on the right-hand side of (A.3) can be bounded by

$$\begin{aligned}
&-\xi^{n+1}\big(\|\mathbf{m}(t^{k+1})\times\Delta\mathbf{m}(t^{k+1})\|^2-\|B_l(\mathbf{m}^k)\times\Delta\tilde{\mathbf{m}}^{k+1}\|^2\big)\\
\le&\xi^{n+1}\|\mathbf{m}(t^{k+1})\times\Delta\mathbf{m}(t^{k+1})+B_l(\mathbf{m}^k)\times\Delta\tilde{\mathbf{m}}^{k+1}\|\|\mathbf{m}(t^{k+1})\times\Delta\mathbf{m}(t^{k+1})-B_l(\mathbf{m}^k)\times\Delta\tilde{\mathbf{m}}^{k+1}\|\\
\le&\xi^{n+1}\|\mathbf{m}(t^{k+1})\times\Delta\mathbf{m}(t^{k+1})+B_l(\mathbf{m}^k)\times\Delta\tilde{\mathbf{m}}^{k+1}\|\|(\mathbf{m}(t^{k+1})-B_l(\mathbf{m}^k))\times\Delta\mathbf{m}(t^{k+1})\|\\
&+\xi^{n+1}\|\mathbf{m}(t^{k+1})\times\Delta\mathbf{m}(t^{k+1})+B_l(\mathbf{m}^k)\times\Delta\tilde{\mathbf{m}}^{k+1}\|\|B_l(\mathbf{m}^k)\times(\Delta\mathbf{m}(t^{k+1})-\Delta\tilde{\mathbf{m}}^{k+1})\|\\
\le&C\xi^{n+1}\|B_l(\mathbf{m}^k)\times\Delta\tilde{\mathbf{m}}^{k+1}\|_{L^2}\|B_l(e^k_{\mathbf{m}})\|_{L^4}\|\Delta\mathbf{m}(t^{k+1})\|_{L^4}\\
&+\xi^{n+1}\|B_l(\mathbf{m}^k)\times\Delta\tilde{\mathbf{m}}^{k+1}\|_{L^2}\|B_l(\mathbf{m}^k)\|_{L^\infty}\|\Delta\tilde{e}^{k+1}_{\mathbf{m}}\|_{L^2}\\
&+C\|\Delta\mathbf{m}(t^{k+1})\|_{L^\infty}\|\Delta\tilde{e}^{k+1}_{\mathbf{m}}\|_{L^2}+C\|\sum_{i=1}^{l}d_i\int_{k+1-i}^{k+1}(t^{k+1-i}-s)^{l-1}\frac{\partial^l\mathbf{m}}{\partial t^l}(s)ds\|_{H^1}.
\end{aligned}\tag{A.4}$$

The second term on the right-hand side of (A.3) can be estimated by

$$\begin{aligned}
&-R(t^{k+1})\left(\frac{1}{E(\mathbf{m}(t^{k+1}))+1}-\frac{1}{E(\tilde{\mathbf{m}}^{k+1})+1}\right)\|\mathbf{m}(t^{k+1})\times\Delta\mathbf{m}(t^{k+1})\|^2\\
&\le C\|\mathbf{m}(t^{k+1})\times\Delta\mathbf{m}(t^{k+1})\|^2(\|\nabla\tilde{\mathbf{m}}^{k+1}\|^2-\|\nabla\mathbf{m}(t^{k+1})\|^2)\\
&\le C\|\mathbf{m}(t^{k+1})\times\Delta\mathbf{m}(t^{k+1})\|^2(\|\nabla\tilde{\mathbf{m}}^{k+1}\|+\|\nabla\mathbf{m}(t^{k+1})\|)\|\nabla\tilde{e}^{k+1}_{\mathbf{m}}\|.
\end{aligned}\tag{A.5}$$

Combining (A.3) with (A.4) and (A.5), and taking the inner product with $2\Delta t e_R^{k+1}$ result in

$$\begin{aligned}
&(|e_R^{k+1}|^2-|e_R^k|^2+|e_R^{k+1}-e_R^k|^2)+2\Delta t\frac{\|\mathbf{m}(t^{k+1})\times\Delta\mathbf{m}(t^{k+1})\|^2}{E(\tilde{\mathbf{m}}^{k+1})+K_0}|e_R^{k+1}|^2\\
\le&C\Delta t\xi^{n+1}\|B_l(\mathbf{m}^k)\times\Delta\tilde{\mathbf{m}}^{k+1}\|^2(\|B_l(\tilde{e}^k_{\mathbf{m}})\|_{L^2}\|\nabla B_l(\tilde{e}^k_{\mathbf{m}})\|_{L^2}+(C_0\Delta t)^{2q})\\
&+\frac{1}{4M_T}\xi^{n+1}\Delta t\|B_l(\mathbf{m}^k)\times\Delta\tilde{\mathbf{m}}^{k+1}\|^2\|B_l(\mathbf{m}^k)\|^2_{L^\infty}|e_R^{k+1}|^2+C_3\Delta t|e_R^{k+1}|^2\\
&+C\Delta t\xi^{n+1}\|\Delta\tilde{e}^{k+1}_{\mathbf{m}}\|^2_{L^2}+C(\Delta t)^{2l}\int_{k+1-l}^{k+1}\|\frac{\partial^l\mathbf{m}}{\partial t^l}(s)\|^2_{H^1}ds+C(\Delta t)^3.
\end{aligned}\tag{A.6}$$

Summing (A.6) over k, $k=0,1,2,\dots,n^*$, where n^* is the time step at which $|e_R^{n^*+1}|$ achieves its maximum value for $k=0,1,2,\dots,n$, we can obtain

$$\begin{aligned}
|e_R^{n^*+1}|^2\le&\frac{1}{4M_T}|e_R^{n^*+1}|^2\sum_{k=0}^{n^*}\Delta t\xi^{n+1}\|B_l(\mathbf{m}^k)\times\Delta\tilde{\mathbf{m}}^{k+1}\|^2\|\tilde{\mathbf{m}}^k\|^2_{L^\infty}\\
&+C\sum_{k=0}^{n^*}\Delta t\xi^{n+1}\|B_l(\mathbf{m}^k)\times\Delta\tilde{\mathbf{m}}^{k+1}\|^2\|B_l(\tilde{e}^k_{\mathbf{m}})\|^2_{L^2}\\
&+C\sum_{k=0}^{n^*}\Delta t\xi^{n+1}\|B_l(\mathbf{m}^k)\times\Delta\tilde{\mathbf{m}}^{k+1}\|^2\|\nabla B_l(\tilde{e}^k_{\mathbf{m}})\|^2_{L^2}+C\sum_{k=0}^{n^*}\Delta t\|\Delta\tilde{e}^{k+1}_{\mathbf{m}}\|^2_{L^2}\\
&+C_3\sum_{k=0}^{n^*}\Delta t|e_R^{k+1}|^2+C(\Delta t)^{2l}\int_0^T\|\frac{\partial^l\mathbf{m}}{\partial t^l}(s)\|^2_{H^1}ds+C(C_0\Delta t)^{2q}+C(\Delta t)^2.
\end{aligned}\tag{A.7}$$

Thus choosing $\Delta t\le\frac{1}{2C_3}$ and using the discrete Gronwall lemma, we can obtain the desired result (A.1). □

References

[1] B. Guo, M.-C. Hong, The landau-lifshitz equation of the ferromagnetic spin chain and harmonic maps, Calc. Var. Partial. Differ. Equ. 1 (1993) 311–334.
[2] L. Landau, E. Lifshitz, On the theory of the dispersion of magnetic permeability in ferromagnetic bodies, in: Perspectives in Theoretical Physics, Elsevier, 1992, pp. 51–65.
[3] Y. Cai, J. Chen, C. Wang, C. Xie, A second-order numerical method for landau-lifshitz-gilbert equation with large damping parameters, J. Comput. Phys. 451 (2022) 110831.
[4] C. Xie, C.J. García-Cervera, C. Wang, Z. Zhou, J. Chen, Second-order semi-implicit projection methods for micromagnetics simulations, J. Comput. Phys. 404 (2020) 109104.
[5] M. Kruzik, A. Prohl, Recent developments in the modeling, analysis, and numerics of ferromagnetism, SIAM Rev. 48 (3) (2006) 439–483.
[6] M. Lakshmanan, K. Nakamura, Landau-lifshitz equation of ferromagnetism: exact treatment of the gilbert damping, Phys. Rev. Lett. 53 (26) (1984) 2497.
[7] Q. Cheng, J. Shen, Length preserving numerical schemes for landau–lifshitz equation based on lagrange multiplier approaches, SIAM J. Scientific Comput. 45 (2) (2023) A530–A553.
[8] W. E, X.-P. Wang, Numerical methods for the landau-lifshitz equation, SIAM J. Numer. Anal. (2001) 1647–1665.
[9] F. Alouges, P. Jaisson, Convergence of a finite element discretization for the landau–lifshitz equations in micromagnetism, Math. Models Methods Appl. Sci. 16 (02) (2006) 299–316.
[10] H. Gao, Optimal error estimates of a linearized backward euler FEM for the landau–lifshitz equation, SIAM J. Numer. Anal. 52 (5) (2014) 2574–2593.
[11] R. An, H. Gao, W. Sun, Optimal error analysis of euler and crank–nicolson projection finite difference schemes for landau–lifshitz equation, SIAM J. Numer. Anal. 59 (3) (2021) 1639–1662.

[12] G. Akrivis, M. Feischl, B. Kovács, C. Lubich, Higher-order linearly implicit full discretization of the landau–lifshitz–gilbert equation, Math. Comput. 90 (329) (2021) 995–1038.
[13] X. Gui, B. Li, J. Wang, Convergence of renormalized finite element methods for heat flow of harmonic maps, SIAM J. Numer. Anal. 60 (1) (2022) 312–338.
[14] F. Pistella, V. Valente, Numerical stability of a discrete model in the dynamics of ferromagnetic bodies, Numer. Methods Partial Differ. Eqs.: Int. J. 15 (5) (1999) 544–557.
[15] A. Prohl, et al., Computational micromagnetism, Springer, 2001.
[16] S. Badia, F. Guillén-González, J.V. Gutiérrez-Santacreu, Finite element approximation of nematic liquid crystal flows using a saddle-point structure, J. Comput. Phys. 230 (4) (2011) 1686–1706.
[17] C. Liu, N.J. Walkington, Approximation of liquid crystal flows, SIAM J. Numer. Anal. 37 (3) (2000) 725–741.
[18] S. Bartels, J. Ko, A. Prohl, Numerical analysis of an explicit approximation scheme for the landau-lifshitz-gilbert equation, Math. Comput. 77 (262) (2008) 773–788.
[19] E. Kim, K. Lipnikov, The mimetic finite difference method for the landau–lifshitz equation, J. Comput. Phys. 328 (2017) 109–130.
[20] R. An, W. Sun, Analysis of backward euler projection FEM for the landau–lifshitz equation, IMA J. Numer. Anal. 42 (3) (2022) 2336–2360.
[21] Y. Cai, J. Chen, C. Wang, C. Xie, Error analysis of a linear numerical scheme for the landau–lifshitz equation with large damping parameters, Math. Methods Appl. Sci. 46 (18) (2023) 18952–18974.
[22] F. Alouges, A new finite element scheme for landau-lifchitz equations, Discrete Contin. Dynam. Syst. Series S 1 (2) (2008) 187–196.
[23] F. Alouges, E. Kritsikis, J. Steiner, J.-C. Toussaint, A convergent and precise finite element scheme for landau–lifschitz–gilbert equation, Numerische Mathem. 128 (3) (2014) 407–430.
[24] F. Alouges, E. Kritsikis, J.-C. Toussaint, A convergent finite element approximation for landau–lifschitz–gilbert equation, Physica B: Condensed Matter 407 (9) (2012) 1345–1349.
[25] F. Huang, J. Shen, A new class of implicit–explicit BDFk SAV schemes for general dissipative systems and their error analysis, Comput. Methods Appl. Mech. Eng. 392 (2022) 114718.
[26] F. Lin, C. Wang, The analysis of harmonic maps and their heat flows, World Scientific, 2008.
[27] J. Shen, Long time stability and convergence for fully discrete nonlinear galerkin methods, Appl. Anal. 38 (4) (1990) 201–229.
[28] Y. He, W. Sun, Stability and convergence of the crank–nicolson/adams–bashforth scheme for the time-dependent navier–stokes equations, SIAM J. Numer. Anal. 45 (2) (2007) 837–869.
[29] J. Shen, X. Yang, Numerical approximations of allen-cahn and cahn-hilliard equations, Discrete Contin. Dyn. Syst. 28 (4) (2010) 1669–1691.
[30] L. Wang, H. Yu, On efficient second order stabilized semi-implicit schemes for the cahn–hilliard phase-field equation, J. Sci. Comput. 77 (2) (2018) 1185–1209.
[31] X.-P. Wang, C.J. Garcıa-Cervera, W. E, A gauss–seidel projection method for micromagnetics simulations, J. Comput. Phys. 171 (1) (2001) 357–372.
[32] O. Nevanlinna, F. Odeh, Multiplier techniques for linear multistep methods, Numer. Funct. Anal. Optim. 3 (4) (1981) 377–423.
[33] F. Huang, J. Shen, Stability and error analysis of a class of high-Order IMEX schemes for navier–stokes equations with periodic boundary conditions, SIAM J. Numer. Anal. 59 (6) (2021) 2926–2954.
[34] K. Cheng, C. Wang, S.M. Wise, Y. Wu, A third order accurate in time, BDF-type energy stable scheme for the cahn-hilliard equation, Numer. Math.: Theory, Methods Appl. 15 (2) (2022).
[35] Y. Hao, Q. Huang, C. Wang, A third order BDF energy stable linear scheme for the no-slope-selection thin film model, Commun. Comput. Phys. 29 (3) (2021).
[36] F. Huang, J. Shen, On a new class of BDF and IMEX schemes for parabolic type equations, SIAM J. Numer. Anal. 62 (4) (2024) 1609–1637.
[37] Y. Gui, R. Du, C. Wang, A third-order implicit-explicit runge-kutta method for landau-lifshitz equation with arbitrary damping parameters, Numer. Math.: Theory, Methods Appl. 17 (4) (2024).
[38] Y. Gui, C. Wang, J. Chen, Implicit-explicit runge-kutta methods for landau-lifshitz equation with arbitrary damping, Commun. Math. Sci. (2024).
[39] Y. Chen, F.H. Lin, Evolution equations with a free boundary condition, J. Geometric Anal. 8 (1998) 179–197.
[40] G. Anzellotti, S. Baldo, A. Visintin, Asymptotic behavior of the landau-lifshitz model of ferromagnetism, Appl. Math. Optim. 23 (1991) 171–192.
[41] P. Li, C. Xie, R. Du, J. Chen, X. Wang, Two improved gauss-seidel projection methods for landau-lifshitz-gilbert equation, J. Comput. Phys. 401 (2020) 109046.
[42] Q.-A. Huang, W. Jiang, J.Z. Yang, C. Yuan, A weighted scalar auxiliary variable method for solving gradient flows: bridging the nonlinear energy-Based and lagrange multiplier approaches, J. Sci. Comput. 106 (1) (2026) 16.
[43] J.-G. Liu, R. Pego, Stable discretization of magnetohydrodynamics in bounded domains, Commun. Math. Sci. 8 (1) (2010) 235–251.